

**LANIER FILTER PLANT  
TREATMENT PROCESS AND DISTRIBUTION SYSTEM STUDY**

**FINAL REPORT**

---

*Submitted to*

**Gwinnett County Public Works**

*By*

**Jaehong Kim, Ph.D.**

School of Civil and Environmental Engineering  
Georgia Institute of Technology  
200 Bobby Dodd Way, Atlanta, GA 30332-0373  
Phone: 404-894-2216  
Fax: 404-894-8266  
Email: jaehong.kim@ce.gatech.edu

**Yonggyun Park, Ph.D.**

CH2MHILL  
Phone: 404-385-7174  
Fax: 404-894-8266  
Email: ypark@ch2m.com

**James E. Amburgey, Ph.D.**

Department of Civil Engineering  
The University of North Carolina at Charlotte  
9201 University City Blvd.  
Charlotte, NC 28223  
Phone: 704-687-6550  
Fax: 704-687-6953  
Email: jeamburg@uncc.edu

October 10<sup>th</sup>, 2006

## TABLE OF CONTENTS

TABLE OF CONTENTS.....	2
LIST OF TABLES.....	4
LIST OF FIGURES .....	5
ACKNOWLEDGMENTS .....	7
EXECUTIVE SUMMARY .....	8
<b>PART I. DISINFECTION BY-PRODUCT FORMATION IN GWINNETT COUNTY'S DRINKING WATER DISTRIBUTION SYSTEM.....</b>	<b>9</b>
1. INTRODUCTION .....	10
1.1. Stage 2 Disinfectant/Disinfection By-Product Rule .....	11
1.2. Water Treatment Process in Gwinnett County .....	13
1.3. Project Objectives .....	15
2. MATERIALS AND METHODS.....	16
2.1. Tracer Test .....	16
2.2. Field Measurements .....	17
2.3. Batch Kinetic Experiments .....	17
2.4. Analytical Methods.....	18
2.5. Gwinnett County Distribution System Model .....	19
3. RESULT AND DISCUSSION .....	22
3.1. Tracer Test .....	22
3.2. Field Measurements .....	31
3.3. Batch Kinetic Study .....	45
3.4. Water Quality Simulation .....	47
4. CONCLUSIONS.....	52
<b>PART II. DEVELOPING A NOVEL OZONE- MEMBRANE HYBRID PROCESS FOR LANIER FILTER PLANT .....</b>	<b>54</b>
1. INTRODUCTION .....	55
2. MATERIALS AND METHODS.....	57
2.1. Feed Water .....	57

2.2. Membranes.....	57
2.3. Cross-Flow Filtration Experiments.....	57
2.4. Membrane Cleaning.....	60
2.5. Analytical Methods.....	60
3. RESULT AND DISCUSSION .....	61
4. CONCLUSIONS.....	65
5. REFERENCES .....	66

## LIST OF TABLES

Table 1. MCLGs and MCLs for DBPs according to Stage 2 D/DBPR .....	11
Table 2. Reviews of Stage 1 and 2 D/DBPRs .....	13
Table 3. Summary of the pipelines sorted by their diameter .....	19
Table 4. Sampling locations of Tracer Test I.....	22
Table 5. Sampling locations of Tracer Test II.....	26
Table 6. Sampling locations of field measurements .....	31
Table 7. Water quality parameters measured.....	33
Table 8. Observed finished water parameters .....	35
Table 9. Characteristics of LFP source water used in this study .....	57
Table 10. Permeate flux at each stage.....	63

## LIST OF FIGURES

Figure 1. Comparing DBP monitoring methods in Stage 1 and Stage 2 D/DBPR.....	12
Figure 2. Water Distribution System of Gwinnett County .....	21
Figure 3. An example of fluoride concentration decrease during the tracer test and estimating water age. ....	23
Figure 4. Comparing water age with residual chlorine determined from the tracer test I.....	24
Figure 5. Water age simulation results obtained using field conditions for the tracer test I.....	25
Figure 6. Comparing water ages estimated using the model and measured during the first tracer test.....	26
Figure 7. Comparing water age with residual chlorine determined from the tracer test II. ....	28
Figure 8. Water age simulation results obtained using field conditions for the tracer test II. ....	29
Figure 9. Comparing water ages estimated using the model and measured during the first tracer test.....	30
Figure 10. Residual chlorine, TTHM, and HAA5 concentrations obtained from the field measurement.....	36
Figure 11. Comparing differential TTHM concentration and differential residual chlorine. ....	38
Figure 12. Comparing differential HAA5 concentration and differential residual chlorine .....	39
Figure 13. Comparing differential THM concentration and differential residual chlorine .....	40
Figure 14. HAA species concentration vs. residual chlorine concentration .....	41

Figure 15. TOC vs. TTHM or HAA5 concentration .....	43
Figure 16. DOC vs. TTHM or HAA5 concentration .....	43
Figure 17. UV <sub>254</sub> vs. TTHM or HAA5 concentration .....	44
Figure 18. SUVA vs. TTHM or HAA5 concentration .....	44
Figure 19. Kinetics of residual chlorine decay at 25°C in a laboratory batch experiment .....	45
Figure 20. Kinetics of TTHM formation at 25°C in a laboratory batch experiment .....	46
Figure 21. Kinetics of HAA5 formation at 25°C in a laboratory batch experiment .....	47
Figure 22. Model simulation of residual chlorine concentration in the Gwinnett County water distribution system (under the condition for the date of field experiment) .....	49
Figure 23. Comparing residual chlorine measured in the field and predicted with the model .....	50
Figure 24. Comparing TTHM measured in the field and predicted with the model .....	51
Figure 25. Comparing HAA5 measured in the field and predicted with the model .....	51
Figure 26. Schematic of Crossflow Filtration Experimental Setup .....	58
Figure 27. Photographs of Experimental Setup .....	59
Figure 28. Permeate fluxes of ceramic membranes treating ozone contactor influent and effluent .....	61
Figure 29. Total organic carbon in membrane feed and permeate. ....	62
Figure 30. Specific UV absorbance of membrane feed and permeate .....	62
Figure 31. The calculated resistances of two membranes from resistance in series model .....	64

## **ACKNOWLEDGMENTS**

The authors gratefully acknowledge supports by Mr. Neal C. Spivey (Public Utilities, Gwinnett County, GA), Dr. Robert (Bob) Faro (Public Utilities, Gwinnett County, GA), Dr. Yong-Mo Cho (Seoul Development Institute), Mr. Richard R. Elliott (MWH), Mr. Dooil Kim (Georgia Institute of Technology), and Dr. Guangxuan Zhu (Georgia Institute of Technology). Special thanks go to Envirosoft Engineering & Science Inc. for the updated distribution system model and Underwriters Laboratories Inc. for the analysis of THMs and HAAs. The project tasks were performed when Yonggyun Park, currently at Ch2MHill, was a graduate research assistant at Georgia Institute of Technology.

## EXECUTIVE SUMMARY

This report summarizes the outcome of the project funded by Gwinnett County Public Utilities and performed by Georgia Institute of Technology during the period August 2004 to August 2006. The project was composed of two parts. The Part I of the project focused on evaluating occurrence of disinfection by-products such as THMs and HAAs at Lanier Filter Plant (LFP) effluent and various locations in Gwinnett County Water Distribution System, to which the LFP is currently serving its water. A network model based on WaterGEMS was used to predict the water age, residual chlorine and DBP levels in consumer taps throughout the distribution system. Experimental data obtained from the field-scale tracer tests and water quality studies suggested that the model provided a very useful tool to simulate the performance of distribution system, in compliance with the EPA's Initial Distribution System Evaluation (IDSE) requirement of the Stage 2 Disinfectant / Disinfection By-Product Rule (D/DBPR). Experimental and modeling data suggested that water age was an important indicator to determine water quality in terms of both chlorine residual and TTHM levels in this distribution system. Some regions within the distribution system with the longest retention time and lowest free chlorine residuals were identified from both modeling and field study. Part II of the project involved developing a novel ozone-ultrafiltration membrane hybrid process tailored for the LFP. Bench-scale cross-flow ceramic ultrafiltration experiments performed at the LFP suggested that ozone treatment of raw water did affect the fouling characteristics of ultrafiltration membrane. After ozone treatment, the overall contribution of cake resistance to the total resistance increased, while little difference was observed with the total resistance. However, a direct application of ozone to the fouled membrane was not found to be very effective when compared with commonly used chemical treatment methods. This suggested that irreversible fouling observed with the ceramic membrane might have resulted from pore clogging, which is not easily removed by either mechanical or chemical methods. As the major advantage of using the ceramic membrane is its extremely strong chemical resistance and potential for cleaning by the existing ozonation facility, this suggests that the use of high-cost ceramic membrane might not be justifiable in the LFP.



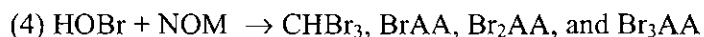
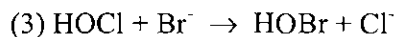
**PART I.**  
**DISINFECTION BY-PRODUCT FORMATION**  
**IN GWINNETT COUNTY'S DRINKING WATER DISTRIBUTION SYSTEM**

## 1. INTRODUCTION

### 1.1. Stage 2 Disinfectant/Disinfection By-Product Rule

A drinking water distribution system can be viewed as a very large and complex reactor in which the quality of finished water changes both spatially and temporally because of physical, chemical, and biological phenomena such as mixing and dispersion, nitrification, disinfectant decay, disinfection by-product (DBP) formation, microbial growth, pathogen intrusion, and corrosion. It has been reported that there are more violations of drinking water standards related to the distribution system than to water treatment. Therefore, more public attention has recently been paid to the quality of water at consumers' taps and its dependence on distribution system network and operation.

In the United States, most drinking water treatment utilities use residual disinfectants such as free chlorine and monochloramine in order to suppress microbial activity during water distribution. However, these residual disinfectants react with organic matter present in the treated water to produce chlorinated DBPs such as trihalomethanes (THMs), haloacetic acids (HAAs), haloacetonitriles (HANs), haloketones (HKs), and chloropicrin (CP), among many others (Chen and Weisel, 1998). Because finished water travels for a considerable amount of time in the distribution system in the presence of reactive residual disinfectants, DBP levels at consumers' taps are typically two to three times higher than those in water treatment plant effluents (Rossman et al., 2001). The reactions governing the formations of the various THMs and HAAs are as follows:



It is well known from several toxicological and epidemiological studies that halogenated DBPs such as THMs and HAAs have severe effects on human health. Examples of adverse health effects include colon, rectal, bladder, and liver cancer development and adverse reproductive outcomes such as low birth weight, preterm delivery, spontaneous abortion, stillbirth, and birth defects (Pereira et al. 2004).

Therefore, regulations dealing with DBPs have been continuously becoming more stringent over the past decades in order to increase public safety related to drinking water. Most recently, Stage 2 Disinfectant and Disinfection By-Product Rule (Stage 2 D/DBPR) was promulgated in January, 2006, placing upper limits on chlorination DBPs (TTHM and HAA5) and alternative DBPs (bromate and chlorite) in finished and tap waters. Under this regulation, it is also required for all the water utilities to develop a system-specific Initial Distribution System Evaluation (IDSE) program. The specifics of the IDSE study varies depending on the sizes of distribution system and the population served. The maximum contaminant level goals (MCLGs) and the maximum contaminant levels (MCLs) of the DBPs in the current Stage 2 D/DBPR are listed in the Table 1.

Table 1. MCLGs and MCLs for DBPs according to Stage 2 D/DBPR

<i>Disinfection By-Products</i>	<i>MCLG (mg/L)</i>	<i>MCL (mg/L)</i>
Total trihalomethanes	N/A	0.080
Haloacetic acids (HAA5)	N/A	0.060
Chlorite	0.8	1.0
Bromate	Zero	0.010

MCLG: Maximum contaminant level goal, MCL: Maximum contaminant level

A notable difference between the Stage 1 and Stage 2 D/DBPR is the way to determine regulatory compliance related to DBP levels in the distribution system. To comply with the requirements of the Stage 1 D/DBPR in the past, the utilities used to measure the total concentrations of four trihalomethanes (TTHM) and five haloacetic acids (HAA5) in the

distribution system once each quarter at three locations that would represent average hydraulic residence times (HRTs) and at one location with the highest HRT. The seasonal average DBP levels in the distribution system were used to calculate annual average values which were required to be below the MCLs (80 µg/L for TTHM and 60 µg/L for HAA5) of each DBP. This monitoring method is called Running Annual Average (RAA). Unfortunately, this method failed to regulate situations in which water with very high DBP levels would be consistently served to a specific location and sub-population within the system, as long as the RAA DBP levels in the overall distribution systems was below the MCLs. As a result, Stage 2 D/DBPR requires that average DBP levels in *each* sampling location (called Locational Running Annual Average, LRAA) should be below the MCLs. Figure 1 shows the monitoring methods of TTHM and HAA5 concentrations in Stage 2 compared to Stage 1 D/DBPRs. Additional comparison between these regulations are provided in Table 2.

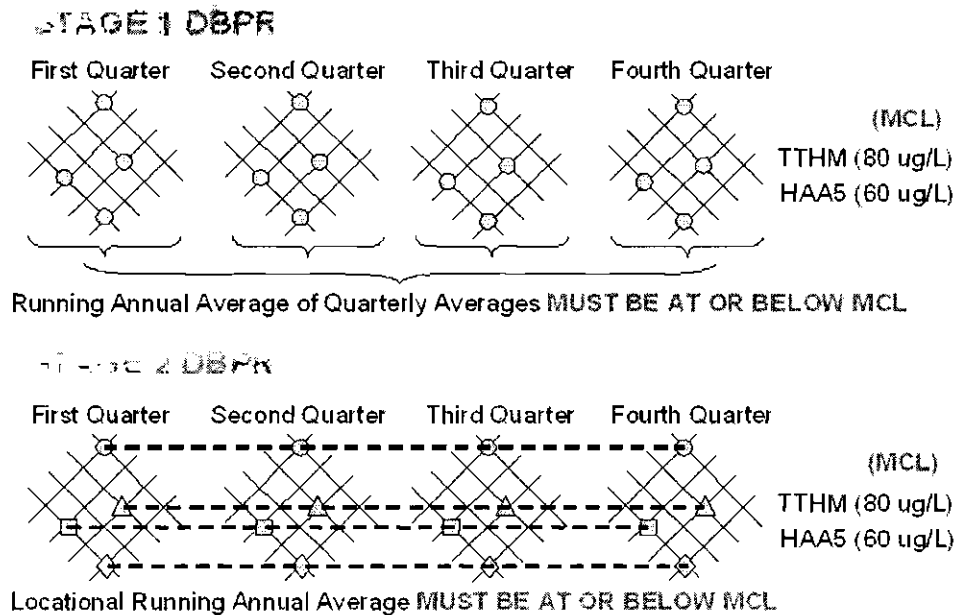


Figure 1. Comparing DBP monitoring methods in Stage 1 and Stage 2 D/DBPR (from *Draft Stage 2 DBPR Implementation Guidance, November 2003*).

Table 2. Reviews of Stage 1 and 2 D/DBPRs (IDSE Manual, 2006)

<i>Stage 1 D/DBPR</i>	<i>Stage 2 D/DBPR</i>
<ul style="list-style-type: none"> <li>• The first staged set of rules designed to reduce allowable levels of DBPs in drinking water.</li> <li>• Compliance dates and frequency of monitoring based on source and population</li> <li>• Number of samples is plant-based</li> <li>• Established maximum residual disinfectant levels (MRDLs) for 3 chemical disinfectants (chlorine, Chloramine, and Chlorine Dioxide)</li> <li>• Established maximum contaminant levels (MCLs) for TTHMs and HAA5's (80 ug/L and 60 ug/L, respectively)</li> <li>• Requires removal of specified percentages of TOC, which may react with disinfectants to form DBPs</li> <li>• Compliance monitoring calculated as a running annual average (RAA) of all monitoring locations across system.</li> </ul>	<ul style="list-style-type: none"> <li>• The second staged set of rules designed to tighten compliance monitoring requirements for TTHMs and HAA5s</li> <li>• Compliance dates are population based and incremental, starting with systems at greatest risk (Schedules 1 - 4)</li> <li>• Requires systems to complete the Initial Distribution System Evaluation (IDSE) to characterize DBP levels in the distribution systems.</li> <li>• IDSE is to identify distribution system locations with high concentrations of TTHM and HAA5.</li> <li>• Standard monitoring results from the IDSE, along with Stage 1 DBPR compliance monitoring, will be used to select compliance monitoring locations for the Stage 2 D/DBPR.</li> <li>• Stage 2 compliance monitoring will be calculated for each monitoring location (approach known as LRAA)</li> </ul>

## 1.2. Water Treatment Process in Gwinnett County

Gwinnett County currently operates two water treatment plants: Lanier Filter Plant (LFP) and Shoal Creek Filter Plant (SCFP), both treating Lake Sydney Lanier water. The LFP was constructed between 1975 and 1977, originally as a conventional water treatment plant with a rated capacity of 20 million gallons per day (MGD). During the expansion in 1983, the facility

was converted to a direct filtration plant and the capacity was increased to 100 MGD. A subsequent expansion in 1997 increased the treatment capacity to 150 MGD and incorporated a new pre-ozonation process. The SCFP with a capacity of 75 MGD was constructed in 2004 based on the treatment scheme that is the same as the one currently in use at the LFP. The treated water from SCFP is delivered to the LFP, combined with the treated water from the LFP, and pumped through the distribution system.

The first treatment step is the addition of ozone for primary disinfection. The ozone facility has four 100,000-gallon contactors, and is designed for a 0.5-0.6 log removal of *Giardia lamblia* cysts. A typical ozone dose is 1.0 mg/L and the contact time is at least 4 min. Up to 1,5000 pounds per day of ozone is generated on-site from liquid oxygen. Once the ozone gas is generated, it is introduced into the flow stream using a patented side-stream venturi injection process. Ozone contactor effluent is then directed to the rapid mix tank which has four separate trains, with each train consisting of two 8,480-gallon tanks placed in series. Ferric chloride is added as a primary coagulant at a typical dose of 0.5 mg/L in the first stage and the cationic polymers as a coagulant aid at a typical dose of 1.5 mg/L in the second stage. Flocculation process is accomplished in the flocculation basin which consists of four separate trains. Each train consists of three 69,275-gallon tanks. The flocculated water is then treated by the dual media filters. There are 12 deep bed filters with an area of 1,176 square feet each. The filter media consist of 48 inches of anthracite coal (with effective size of 1.5 mm and a uniformity coefficient of 1.3) and 12 inches of sand (with an effective size of 0.7 mm and a uniformity coefficient of 1.4). The filters are operated at a maximum rate of 7.4 gpm/ft<sup>2</sup>. The last step in the treatment process is the final chemical addition. Free chlorine is added at a typical dose of 2.0 mg/L as Cl<sub>2</sub> to maintain a residual throughout the distribution system. In addition, fluoride is added at *ca.* 1.0 mg/L for tooth decay prevention, liquid lime to adjust the pH, and 50% orthophosphate / 50% polyphosphate blend at *ca.* 2.5 mg/L for corrosion control. The treated water flows into the Clear Wells, which have a total capacity of approximately 19.2 million gallons, and then to a high service pump station for discharge into the distribution system. The distribution system consists of over 3,100 miles of water mains, with sizes ranging from 108-inch transmission mains down to 2-inch house lines.

### **1.3. Project Objectives**

A model to predict water quality in a distribution system can be extremely useful to support water supply planning, operations, and research as well as to assess problems and potential vulnerabilities with regards to water quality and aesthetics (Harding and Walski, 2000). The development of more user-friendly water quality modeling tools and techniques also enabled water treatment facilities to comply with water quality regulations such as IDSE requirement according to Stage 2 D/DBPR. Accordingly, the main objective of this research was to evaluate trihalomethane (THMs) and haloacetic acid (HAAs) levels in the Gwinnett County water distribution system in order to develop an Initial Distribution System Evaluation (IDSE) as required by Stage 2 D/DBPR. A distribution system model based on commercial software, WaterGEMS, which had previously been developed by the county and calibrated by Envirosoft Engineering & Science Inc., was used to estimate the concentrations of residual chlorine, THMs, and HAAs in the distribution system. Tracer tests and field measurements were performed to examine the water quality in the distribution system and to evaluate the model provided by the county. Additional water quality parameters including TOC, DOC,  $UV_{254}$ , SUVA, pH, temperature, conductivity, iron concentration and HPC were also measured to investigate how those parameters affect DBP formation as well as residual chlorine decay. Batch kinetic studies were also conducted to estimate the kinetics of chlorine residual decay and DBP formation.

## **2. MATERIALS AND METHODS**

The project consisted of three major steps: (1) field scale data collection from distribution system, (2) batch kinetic experiments for determination of residual chlorine decay and DBP formation kinetics, and (3) computer simulation of water age, residual chlorine, TTHM and HAA5. The data collection included two tracer tests performed to estimate water age at several sampling locations. The results from the tracer tests were used to validate the hydraulic model with WaterGEMS. Water quality parameters such as pH and residual chlorine concentration were analyzed in the field, while water samples separately preserved for laboratory analysis of the other parameters such as conductivity, TOC, DOC, UV<sub>254</sub>, SUVA, HPC, iron concentration and so forth, which are known indicators of water quality. The batch kinetic study included analysis of residual chlorine decay rate and DBP formation rate within a certain period of time as well as the formation potential of THMs and HAAs under laboratory conditions. The kinetic data obtained were used later to calculate residual chlorine and DBP levels by computational modeling with WaterGEMS.

### **2.1. Tracer Tests**

The formation of disinfection by-products (DBPs) will generally increase as water age increases, while some DBPs such as HAAs have been known to decrease as water age increases under certain conditions. Such degradation occurs primarily due to microbial activity, which often accompanies the loss of disinfectant residual. Therefore, determining accurate water age is critical for identifying optimal locations for sampling DBPs to ensure compliance with the Stage 2 D/DBPR. Tracer tests were conducted twice in October and December, 2004, in order to validate the distribution system model with respect to water age. The tracer test was initiated by discontinuing fluoride feed, which was continuously added to the treated water at a typical concentration of 1 mg/L. The fluoride concentration was then monitored in several sampling locations in the distribution system, at least once per day for 8 to 12 days. All the field samples were stored at room temperature in 50 mL glass bottles until fluoride concentrations were analyzed at Georgia Institute of Technology using an Ion Chromatography (IC) with a



conductivity detector. After the residual fluoride in the distribution system was completely dissipated, the fluoride feed was restored to the previous level. The results from the two tracer tests were used to validate the existing hydraulic model.

## **2.2. Field Measurements**

A field study was performed to determine the levels of residual chlorine and DBPs throughout the Gwinnett County distribution system during the warmer months (August to September, 2005), when the rates of residual chlorine decay and DBP formation are typically higher than in the cooler months. Water quality parameters such as temperature, pH, conductivity, TOC, DOC, UV<sub>254</sub>, SUVA, HPC and iron concentration were also measured in these samples. The actual results were compared with the water quality model simulation results.

Water samples were taken from fire hydrants or customers' taps. Before collecting samples, water from the hydrants or the taps was discarded for the first *ca.* 10 minutes, until water temperature was stabilized. The water purging ensured that water samples were actually from the distribution system as opposed to stagnant water sitting in taps and hydrants. As sampling was not possible at discharge side of the supply pumps, a water faucet inside the laboratory of the LFP connected to a high service pump, was used to collect a sample representing finished water. THM samples were collected in headspace-free 45 mL vials containing a quenching agent, sealed with PTFE/silicone septums, and stored at 4°C before being transported to an independent laboratory (Underwriters Laboratories, Inc.) for analysis. HAA samples were also collected in headspace-free 45 mL vials containing a quenching agent (ammonium chloride) and sealed with a PTFE/silicone septum. The analysis of HAAs were also performed by the same laboratory.

## **2.3. Batch Kinetic Experiments**

Batch experiments were performed to determine the kinetics of chlorine decay and THM and HAA formation in the treated water. Twenty-four 1-L amber glass bottles were filled with

finished water (after chlorination) from the LFP collected on the same day of the field experiment. Experimental temperature was controlled at 25°C by placing bottles in a water bath to represent the water temperature in summer when the DBP formation rate is relatively high. Samples for both THMs and HAAs were taken periodically over a seven day period at the following times: approximately 12 hours, 1, 2, 3, 4, 5, 6, and 7 days. Note that each bottle represented one data point in each kinetic test. Chlorine residual was also measured each time a sample was taken in order to examine the decay rate of chlorine over time.

## **2.4. Analytical Methods**

Residual free chlorine was measured by the N,N-diethyl-p-phenylenediamine (DPD) colorimetric method using a Hach field kit (Model: Pocket Colorimeter II Test Kit). The method detection limit is 0.02 mg/L for chlorine concentrations from 0.02 to 2 mg/L and 0.1 mg/L for concentrations from 0.1 to 8 mg/L. Analysis of THMs and HAAs were conducted by Underwriters Laboratories and the analytical methods used for THMs and HAAs were EPA 524.2 and EPA 552.2, respectively.

TOC and DOC were measured according to Standard Methods (1998) using a Shimadzu TOC-VWS Analyzer (Tokyo, Japan). Samples were first acidified with hydrochloric acid (HCl) to depress the pH below 2.0 and purged for 5 min to remove inorganic carbon. UV<sub>254</sub> was measured according to method 5910B (Standard method, 1998) using an Agilent G1812AA UV-Vis Spectrophotometer and 1-cm quartz cell. DOC and UV absorbance measurements were made after filtration through pre-rinsed 0.22 µm polyethersulfone filters prior to acidification of the sample following the method 5910B (Standard Methods, 1998). In addition, SUVA was calculated as UV<sub>254</sub> normalized with respect to DOC, multiplied by 100 (in units of L/mg-m). HPC (Heterotrophic Plate Count) was quantified in duplicate using membrane filtration and incubation on R2R media for 48 hours at 35 ± 0.5 °C (Method 9215 D, Standard Methods, 1998). Iron concentration was measured using an Inductively Coupled Plasma Mass Spectrometer-Atomic Emission Spectroscopy (ICP-AES) (Model ICAP 61E Trace Analyzer, Thermo Jarrell Ash, Franklin, MA) equipped with an autosampler. The wavelength used for iron analysis was 259.94 nm. The precision and accuracy of all measurements were evaluated with check

standards, the analysis of replicate samples, and periodic instrument calibration (Archer and Singer, 2006).

## 2.5. Gwinnett County Distribution System Model

Figure 2 shows the model for the Gwinnett County distribution system used in this study. The model included 2 reservoirs, 66 pumps (including high service pumps), 16 tanks (including Clearwells), 41,417 pipes, and 39,337 pipe junctions. The total length of the pipelines is *ca.* 3,047 miles and the diameter of pipes composing the model ranges from 2 inches to 108 inches. The major pipe materials were Asbestos Cement (AC), Cast Iron (CI), Ductile Iron (DI), PVC, and Steel. The summary of the pipelines are presented in the following Table 3.

Table 3. Summary of the pipelines sorted by their diameter

<i>Pipe Diameter (inch)</i>	<i>Number of Pipes</i>	<i>Pipe Diameter (inch)</i>	<i>Number of Pipes</i>
2	148	30	102
3	1	36	96
4	282	48	397
6	5744	54	2
8	25961	60	4
10	1436	72	2
12	4499	78	43
16	2111	80	2
20	42	108	10
24	535		

In the WaterGEMS program, a modeling scenario is defined by the various modeling alternatives including physical demand, initial settings, age, constituent, and so on. The age alternative was used to calculate water age and the constituent alternative for the concentrations of residual chlorine, TTHM and HAA5. Once each scenario was defined, the modeling was performed to simulate the system response for 312-hour (13-day) extended period. The hydraulic time step was 1 hr. For the calculation of residual chlorine and DBP concentrations,

the kinetics were defined based on those of the bulk reaction, which were experimentally determined from the separate batch experiments. The limiting concentrations of TTHM and HAA5 were also obtained from the batch kinetic study. A total demand for each scenario was adjusted by a “Global Adjustment” tool in WaterGEMS based on the SCADA system data obtained for each field study (*i.e.* tracer tests and field measurements). A trial-and-error approach was taken to match the model to the actual conditions on the days of sampling.



### 3. RESULT AND DISCUSSION

#### 3.1. Tracer Tests

##### *Tracer Test I*

Two sets of tracer tests were conducted to validate the accuracy of the existing distribution system model. The first tracer test was performed in October when water consumption rate was relatively high and water temperature ranged from 23°C to 25°C with an average value at 23.7°C. Because of a large water demand, water age through the distribution system was expected to be relatively low. The sampling locations selected for the first tracer test are shown in Table 4.

Table 4. Sampling locations of Tracer Test I

Sampling Site #	Location	Water Temperature
1	Pump Station, Lanier Filter Plant	23°C
2	343 Highway 23, Suwanee, GA 30024	23°C
3	3288 Highway 120, Duluth, GA 30096	24°C
4	3600 Braselton Hwy, Dacula, GA 30019	24°C
5	642 Russell Road, Lawrenceville, GA 30043	23°C
6	4355 Steve Reynolds Blvd. NW, Norcross, GA 30093	25°C
7	2244 Highway 20, Grayson, GA 30017	24°C
8	1900 Five Forks Trickum Rd, Lawrenceville, GA 30044	24°C
9	195 Dacula Road, Dacula, GA 30019	24°C
10	2739 Brooks Road, Dacula, GA 30019	24°C
11	5885 Live Oak Pkwy, Norcross, GA 30093	24°C
12	2326 Lenora Church Rd, Snellville, GA 30078	24°C
13	5550 Spalding Drive, Norcross, GA 30092	23°C
14	3890 Johnson Drive, Snellville, GA 30039	24°C
15	12 Harmony Grove Road, Lilburn, GA 30047	24°C
16	4075 Howell Park Road, Duluth, GA 30096	23°C
17	5320 Mainstream Circle, Norcross, GA 30092	24°C
18	2291 Plantation Court, Lawrenceville, GA 30044	22°C

The water age at each sampling location was estimated by the time required for a 50 percent reduction in tracer concentration ( $t_{50}$ ) since the fluoride injection stopped (Figure 3). Average water age of the water samples collected was 42 hours and most of water ages monitored were less than 3 days. Residual chlorine levels were also measured to investigate the relationship between water age and residual chlorine level. The average residual chlorine concentration was 1.35 mg/L. Residual chlorine concentration decreased as water age increased as shown in Figure 4, while data showed some fluctuation. This relationship can be explained by the residual chlorine decay resulting from its reaction with natural organic matter (NOM) and pipe wall materials in the distribution system.

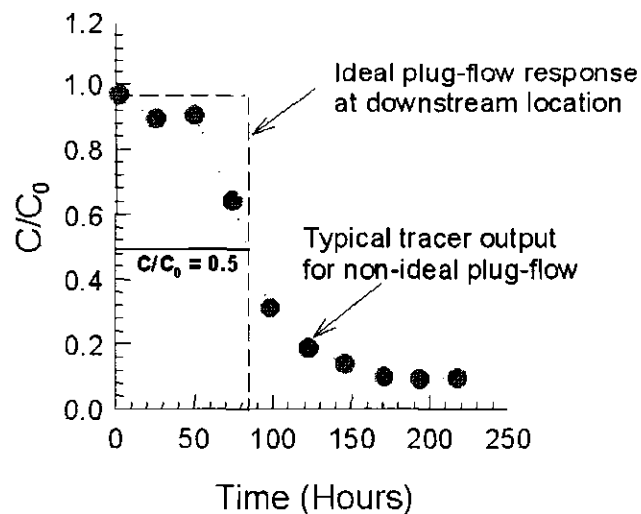


Figure 3. An example of fluoride concentration decrease during the tracer test and estimating water age

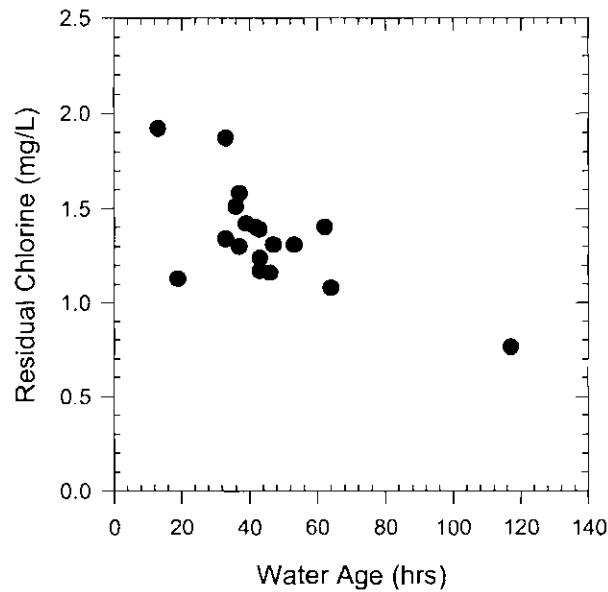


Figure 4. Comparing water age with residual chlorine determined from the tracer test I.

The modeling was performed to simulate the water age using an average daily demand of 66.1 MGD, for an elapsed time of 312 hours at 1-hour increments to achieve an extended period simulation. Figure 5 shows the resulting spatial distribution of water age in color-coded time increment. Most locations in the distribution system have a water age of 96 hours or less. Small pockets of areas throughout the entire distribution system (but more concentrated on the south and east extremities) have water age exceeding 96 hours. Although water age alone does not determine if water is safe or if water quality is acceptable, it is a good indicator of potential concerns, such as low chlorine residual, coliform occurrences, excessive DBP formation and other water quality problems. High water age is often caused by oversized piping, low demands on dead-end water mains, and underutilized storage facilities.



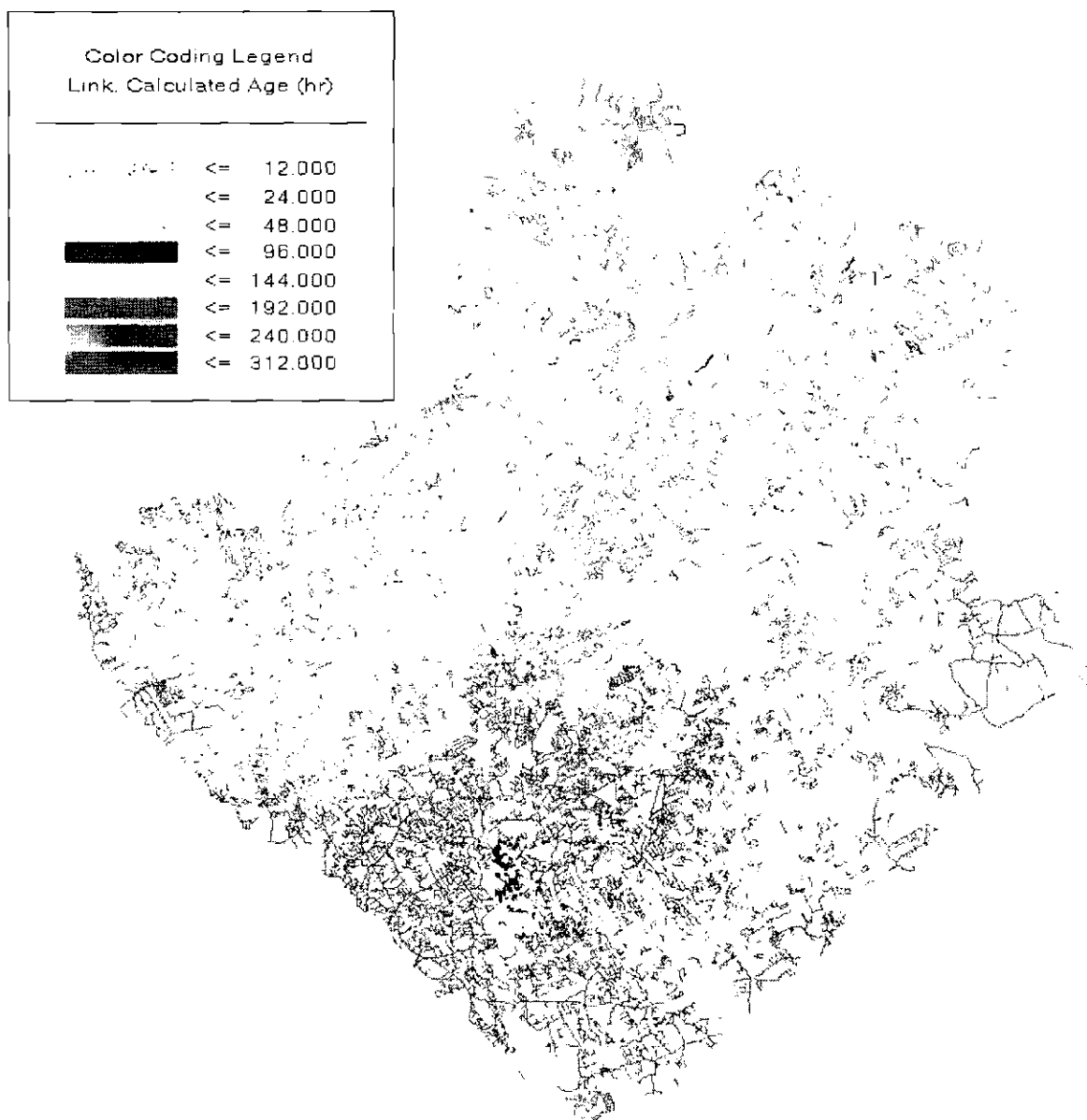


Figure 5. Water age simulation results obtained using field conditions for the tracer test I.

The water ages estimated using the model were compared with those measured during the first tracer test. Figure 6 suggests that the model used in this study is quite accurate in estimating the water age, especially considering the size of the entire system and the many uncertainties that may make model simulations less accurate.

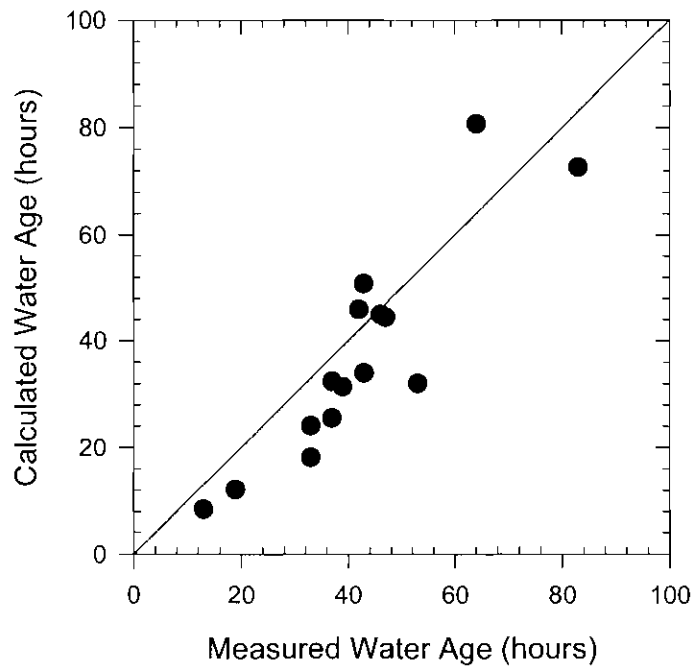


Figure 6. Comparing water ages estimated using the model and measured during the first tracer test.

#### Tracer Test II

Another tracer test was performed in December, 2004 when water demand was *ca.* 55.2 MGD, which was lower than that of the first tracer test. Hence, the water ages were anticipated to be longer than the ones obtained from the first tracer test. Sampling locations were slightly modified in this test, as most samples were collected from the areas relatively far away from the LFP. Selection of these locations was based on the results of the first tracer test. The sampling locations for the second tracer test are presented in Table 5.

Table 5. Sampling locations of Tracer Test II

Sampling Site #	Location	Water Temperature
1	Pump Station, Lanier Filter Plant	14°C
2	2008 Scenic Hwy N Snellville, GA 30078-2151	18°C

3	2622 Club Dr Snellville, GA 30078-3009	16°C
4	3180 Main St W Snellville, GA 30078-7417	18°C
5	4825 Stone Mountain Hwy Lilburn, GA 30047-4643	19°C
6	2699 Stone Dr Sw Lilburn, GA 30047-5723	17°C
7	2463 Broad Creek Dr Stone Mountain, GA 30087-3757	19°C
8	4180 Na Ah Tee Trl Snellville, GA 30039-8066	19°C
9	2750 Riverfront Dr Snellville, GA 30039-8522	19°C
10	5050 Five Forks Trickum Rd Sw Lilburn, GA 30047-5517	19°C
11	4067 Industrial Park Dr Norcross, GA 30071-1638	17°C
12	5300 Spalding Dr Norcross, GA 30092-2605	18°C
13	4901 E Jones Bridge Rd Norcross, GA 30092-1211	18°C
14	4630 River Bottom Dr Norcross, GA 30092-1323	18°C
15	3878 Meadow Creek Dr Norcross, GA 30092-5210	18°C
16	3039 Amwiler Rd Doraville, GA 30360-2824	18°C
17	727 W Peachtree St Norcross, GA 30071-1868	18°C
18	2066 Beaver Ruin Rd Norcross, GA 30071-3763	17°C
19	2099 Kilcrease Rd Bethlehem, GA 30620-4507	17°C
20	2990 Harbins Rd Se Bethlehem, GA 30620-4517	17°C
21	3550 Wapakonata Trl Bethlehem, GA 30620-4645	20°C
22	2499 Snowshoe Bend Se Bethlehem, GA	19°C
23	3225 June Ivey Rd Nw Bethlehem	19°C
24	2734 Michelle Lee Dr Dacula, GA 30019-6917	19°C
25	2490 Brooks Rd Dacula, GA 30019-1951	17°C
26	782 Harbins Rd Dacula, GA 30019-2412	16°C
27	300 Grayson New Hope Rd Grayson, GA 30017-1356	17°C

The water temperature ranged from 14°C to 20°C with an average value at 18°C. Similar to the observation made with the first tracer test, residual chlorine concentration decreased as water age increased. The results obtained are presented in Figure 7, which showed a better relationship between these two parameters compared to the first tracer test results. The average water age was 94 hours and average residual chlorine was 1.28 mg/L. It was not possible to directly compare the residual chlorine levels from two tracer tests because sampling locations

were not the same. While it is expected that water ages are greater in winter due to lower water demand, residual chlorine concentrations might not necessarily be lower as chlorine decay rates also decrease as temperature decrease. For some of common sampling sites, it was often found that chlorine residual was higher even though water age was greater in the second tracer test.

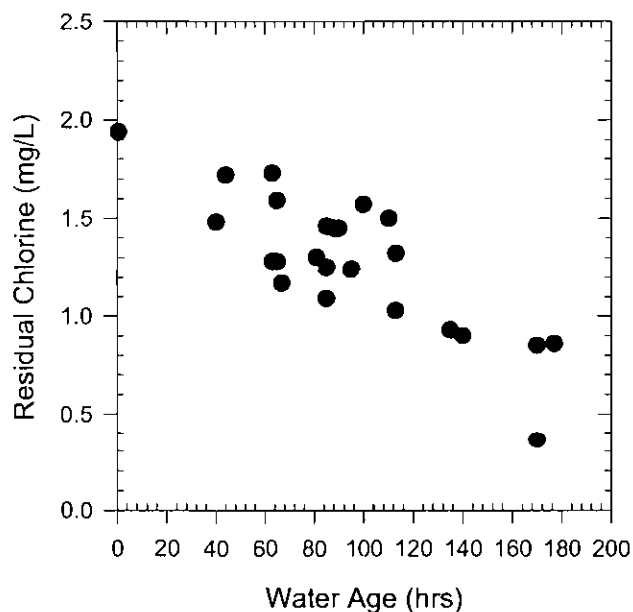


Figure 7. Comparing water age with residual chlorine determined from the tracer test II.

The simulation results using the field conditions that are representative of the second tracer test is presented in Figure 8. Consistent with the previous model simulation, the south and east extremities showed longer water ages, while most of water ages were estimated to be less than 120 hours. The calculated water ages were further compared with the water ages measured from the second tracer test in Figure 9. Once again, the model provided a reasonably good estimation of the field data.

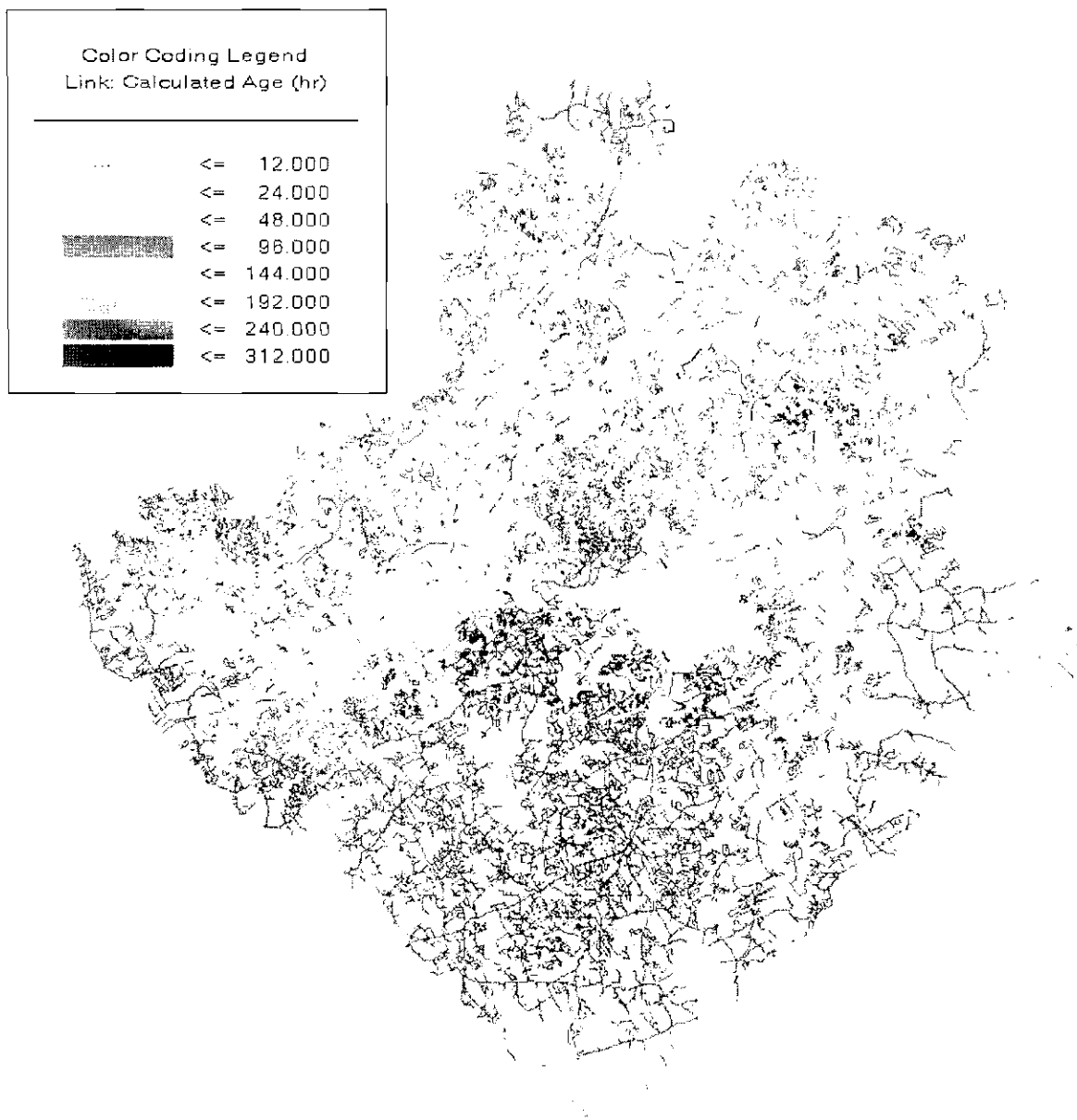


Figure 8. Water age simulation results obtained using field conditions for the tracer test II.

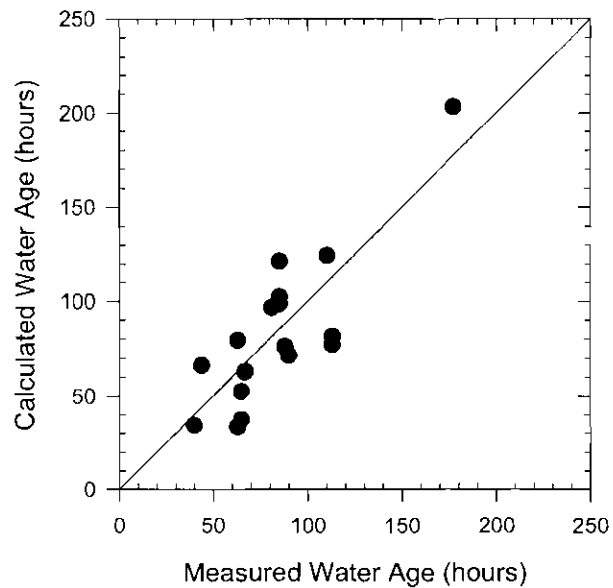


Figure 9. Comparing water ages estimated using the model and measured during the first tracer test.

The following summarizes the findings from the tracer tests and corresponding model simulations:

1. Sampling locations further away from the treatment plant generally showed longer water ages and lower residual chlorine levels. For Gwinnett County, south and east peripheral regions were identified as potential problematic areas.
2. Overall water age determined from the second tracer test was longer than that from the first tracer test due to lower water consumption in winter.
3. The model was reasonably accurate to predict the water age as the results were found fairly comparable to the field data. The modeling result in the second tracer test might have been less accurate, because the retention time was greater (*i.e.* as demand was lower and more sampling locations were further away from the treatment plant).

### 3.2. Field Measurements

Much research has been performed in past decades to develop kinetic models that accurately simulate chlorine decays and DBP formation in distribution systems. However, it has been extremely challenging to develop a mechanistic model for the kinetics because of the complex reactions between chlorine and water constituents. Kinetics are affected by numerous other factors such as temperature, concentration of chlorine residual, reaction time, total organic carbon, bromide content, and so forth (Chen and Weisel, 1998). Therefore, water quality parameters were determined throughout the distribution system in an attempt to identify their effects on chlorine decay and DBP formation. A field study to measure water quality parameters in the distribution was performed in summer (August to September) of 2005. The sampling locations for the field measurement are presented in Table 6. Tables 7 and 8 provide summaries of field study results.

Table 6. Sampling locations of field measurements

Sampling Site #	Location	Water Temperature
1	Raw water (Shoal Creek Filter Plant)	22.9°C
2	Ozonated water (Shoal Creek Filter Plant)	N/A
3	Finished water (Shoal Creek Filter Plant)	25.8°C
4	Raw water (Lanier Filter Plant)	23.9°C
5	Ozonated water (Lanier Filter Plant)	N/A
6	Finished water (Lanier Filter Plant)	24.5°C
7	2045 Beaver Ruin Rd Norcross, GA 30071-3607	22.7°C
8	200 Langford Dr Norcross, GA 30071-1842	23.3°C
9	4630 River Bottom Dr Norcross, GA 30092-1323	26.3°C
10	4901 E Jones Bridge Rd Norcross, GA 30092-1211	25.8°C
11	5300 Spalding Dr Norcross, GA 30092-2605	27.0°C
12	3921 Whitney Pl Duluth, GA 30096-3155 (B)	24.7°C
13	1771 N Oak Dr Lawrenceville, GA 30044-2809	24.6°C
14	2622 Club Dr Snellville, GA 30078-3009	24.7°C
15	2186 Highpoint Rd Snellville, GA 30078-3197	23.7°C

16	2180 Stone Drive, Lilburn, GA 30047 (FS #22)	26.3°C
17	12 Harmony Grove Road, Lilburn, GA 30047 (FS #2)	24.4°C
18	5230 Candleberry Dr Sw Lilburn, GA 30047-6765	25.7°C
19	2463 Broad Creek Dr Stone Mountain, GA 30087-3757	24.1°C
20	3811 Brittan Glade Trl Snellville, GA 30039-8715	23.7°C
21	2845 Lake Port Dr Snellville, GA 30039-5451	27.8°C
22	3610 Cedar Springs Ln Loganville, GA 30052-6686	29.2°C
23	2114 Green Gate Pl Grayson, GA 30017-1858 (B)	27.5°C
24	2739 Brooks Road, Dacula, GA 30019 (FS #17)	24.8°C
25	2971 Harbins Rd Se Bethlehem, GA 30620-4521	25.7°C
26	2470 Snowshoe Bnd Bethlehem, GA 30620-7609	29.2°C
27	3205 June Ivey Rd Nw Bethlehem, GA 30620-4610	28.4°C
28	2734 Michelle Lee Dr Dacula, GA 30019-6917	29.7°C
29	3910 Riversong Ct Suwanee, GA 30024	23.2°C
30	1639 Flowery Branch Rd Auburn, GA 30011-2110	24.5°C
31	1911 Winners Cir Lawrenceville, GA 30043-2789	22.2°C
32	2723 N Bogan Rd Buford, GA 30519-3950	25.0°C



Table 7. Water quality parameters measured.

Sampling Site #	pH	Conductivity (µS/cm)	TOC (mg/L)	DOC (mg/L)	UV <sub>254</sub> (/cm)	SUVA (L/mg/m)	Fe (mg/L)	HPC	Residual Chlorine (mg/L)	TTHM (µg/L)	HAA5 (µg/L)	THMFP (µg/L)	HAAFP (µg/L)
1	6.63	40.7	1.21	1.1	0.0307	2.7903	0.0014	N/A	N/A	N/A	N/A	78.8	79.5
2	N/A	N/A	N/A	N/A	N/A	N/A	N/A	N/A	N/A	N/A	N/A	53.5	53.1
3	7.26	77.4	0.86	0.73	0.0056	0.7622	0.0171	0	1.92	7.9	8.3	50.3	52.4
4	6.66	50.6	1.19	1.06	0.0238	2.2512	0	N/A	N/A	1.8	N/A	78.4	74.7
5	N/A	N/A	N/A	N/A	N/A	N/A	N/A	N/A	N/A	N/A	N/A	58.1	59
6	7.41	81.7	1.22	0.83	0.0066	0.7955	0.003	0	1.91	10.9	10.2	58.5	49.3
7	6.94	78.4	1.29	1.2	0.0074	0.6216	0.0105	2	1.58	15.9	15.4	N/A	N/A
8	7.17	79.8	1.03	0.99	0.0067	0.6705	0.0324	45	1.17	32.5	21.5	N/A	N/A
9	7.48	85.1	0.8	0.8	0.0069	0.8609	0.0132	39	1.56	36.5	26.4	N/A	N/A
10	7.95	82.5	1.14	1.01	0.0061	0.6025	0.2213	3	1.64	29.9	27.8	N/A	N/A
11	10.34	146.9	1.88	0.96	0.0066	0.6866	1.288	1	0.05	73.9	15	N/A	N/A
12	7.82	81.5	1.14	1.06	0.0078	0.7368	0.0933	8	1.93	24.4	16.8	N/A	N/A
13	7.84	81.8	2.35	0.94	0.0065	0.6956	1.525	1	1.52	22.5	20.9	N/A	N/A
14	7.87	82.9	1.03	1.02	0.006	0.5882	0.012	2	0.72	46.8	32.5	N/A	N/A
15	7.64	80.6	1.02	0.98	0.0061	0.6263	0.646	6	1.05	38.9	27	N/A	N/A
16	7.8	85.5	0.98	0.98	0.0082	0.8363	0.0163	11	0.5	45.8	30.2	N/A	N/A
17	7.66	81.7	1.39	0.88	0.0077	0.867	0.0214	0	1.28	22	29.6	N/A	N/A
18	8.03	87.3	1.03	0.98	0.0073	0.7405	0.6524	1	1.42	47.1	41.9	N/A	N/A
19	7.75	82.5	1.02	0.95	0.0072	0.7574	0.0611	1	1.26	30.1	32.5	N/A	N/A
20	7.97	84.1	1	0.96	0.0067	0.6954	0.0387	2	1.07	37.6	40.4	N/A	N/A
21	8.16	86	1.28	1.02	0.0067	0.6582	0.4463	2	1.3	36.6	34.9	N/A	N/A

22	8.32	87.7	1.07	0.99	0.0076	0.7613	0.1251	22	0.98	48.6	36.4	N/A	N/A
23	8.19	84.2	1.35	1.01	0.0072	0.7144	4.872	1	N/A	38.6	37.4	N/A	N/A
24	7.73	82.2	1.02	0.97	0.0077	0.7916	0.0034	0	1.5	22.3	25	N/A	N/A
25	8.1	83.7	1.04	0.88	0.008	0.9077	0.1066	5	1.17	33.2	33.9	N/A	N/A
26	8.64	86.7	1.14	1.05	0.0067	0.6323	0.3642	7	0.95	47.6	40.6	N/A	N/A
27	9.04	89.8	1.1	1.03	0.0068	0.6645	0.0077	11	0.36	70.9	32.1	N/A	N/A
28	10.17	136	1.17	1.16	0.0084	0.7242	0.4278	58	0.31	75.2	29.5	N/A	N/A
29	7.81	83.8	0.97	0.97	0.0066	0.6876	0.0203	1	1.67	16.6	16.9	N/A	N/A
30	7.58	78.9	0.99	0.95	0.0075	0.7868	0.2095	2	1.59	15.5	15.2	N/A	N/A
31	7.37	75.7	1.03	0.85	0.0066	0.7777	0.0152	2	1.73	13	12.1	N/A	N/A
32	7.91	77.2	0.74	0.68	0.0066	0.9752	0.427	175	0.05	55.2	0.0	N/A	N/A

---

Table 8. Observed finished water parameters

Water Quality Parameter	Range	Average / Standard Deviation
pH	6.94 – 10.34	8.03 / 0.75
Conductivity ( $\mu\text{S}/\text{cm}$ )	75.7 – 146.9	87.19 / 15.74
Water Temperature ( $^{\circ}\text{C}$ )	22.2 – 29.7	25.51 / 2.02
TOC ( $\text{mg}/\text{L}$ )	0.74 – 2.35	1.16 / 0.31
DOC ( $\text{mg}/\text{L}$ )	0.68 – 1.20	0.97 / 0.10
UV-254 ( $\text{cm}^{-1}$ )	0.0060 – 0.0084	0.0070 / 0.0006
SUVA ( $\text{L}/\text{mg}/\text{m}$ )	0.6025 – 0.9752	0.74 / 0.09
Residual Chlorine ( $\text{mg}/\text{L Cl}_2$ )	0.05 - 1.91	1.16 / 0.53
TTHM (ppb)	10.9 – 75.2	36.60 / 17.59
HAA5 (ppb)	10.2 – 41.9	27.00 / 9.21

The pH ranged from 7.0 to 8.5 and conductivity from 70 to 90 ( $\mu\text{S}/\text{cm}$ ) in most locations. However, there were two locations that showed abnormally high pH and conductivity: sampling site #11 (pH = 10.34 and conductivity = 146.9  $\mu\text{S}/\text{cm}$ ) and #28 (pH = 10.17 and conductivity = 136  $\mu\text{S}/\text{cm}$ ). Residual chlorine concentrations in those locations were only 0.05 and 0.31  $\text{mg}/\text{L}$ , respectively for sites #11 and #28, which were much lower than most other locations. In contrast, TTHM concentrations were 73.9 and 75.2  $\text{ug}/\text{L}$ , respectively, which were also much higher than the average. It was considered beyond of the scope of this study to understand the reason why these locations showed abnormality, as no other direct water quality parameters showed a clear relationship. The results obtained from the field study are shown in Figure 10 on top of the distribution system map.

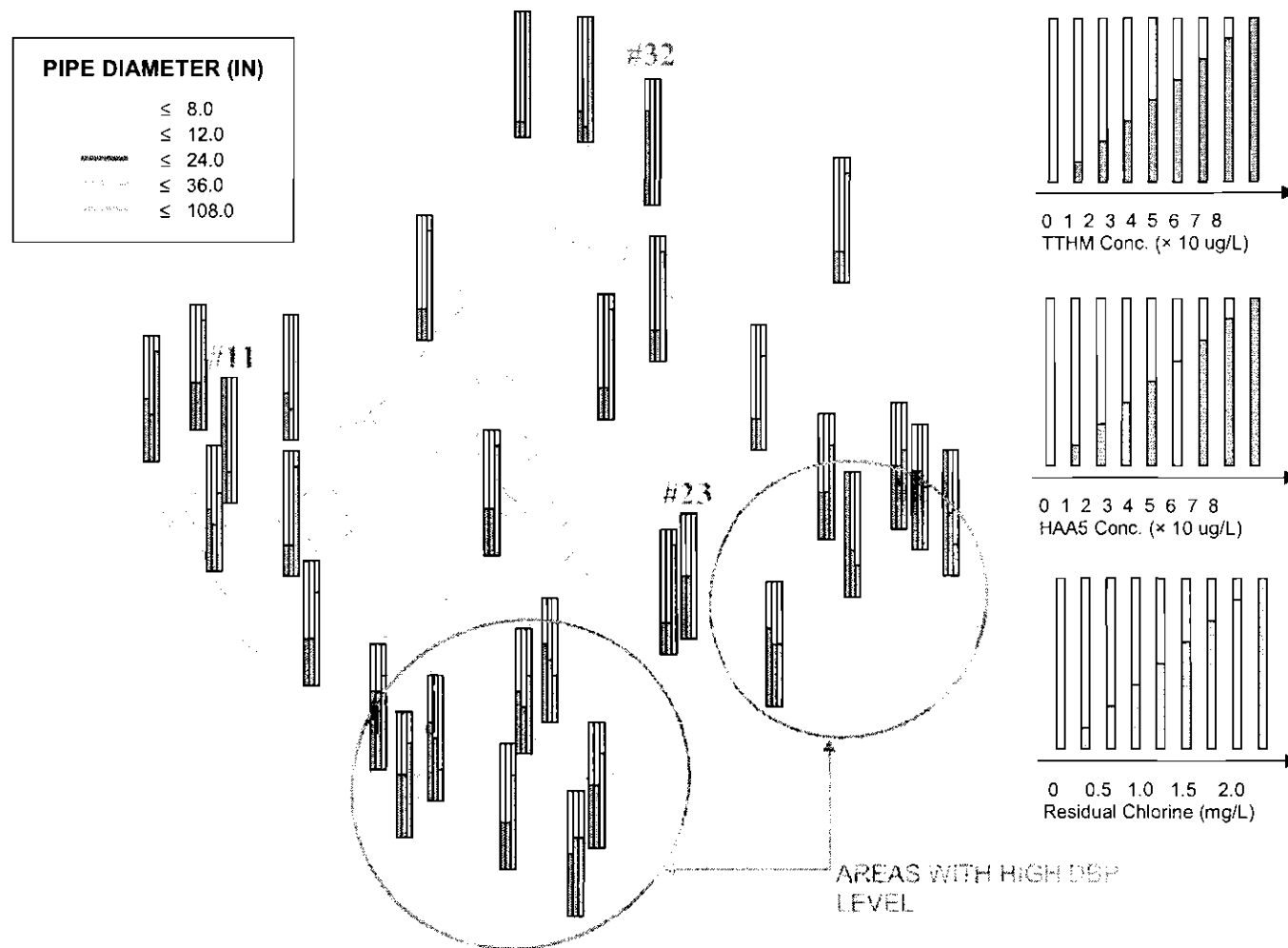


Figure 10. Residual chlorine, TTHM, and HAA5 concentrations obtained from the field measurement.

The average concentrations of residual chlorine, TTHM and HAA5 were measured from the field study at 1.16 mg/L, 36.6 µg/L, and 27.0 µg/L, respectively. As expected from the tracer test results, south and east extremities showed relatively high DBP and low residual chlorine levels. In particular, the residual chlorine concentrations were very low in sampling sites #11, #23, and #32.

Sampling site #11 was located near the Medlock Bridge water storage tank, and the water age was measured at 170 hours according to the second tracer test. Therefore, it might be possible that extended retention time in the storage tank caused the low residual chlorine level (0.05 mg/L) and high TTHM level (73.9 µg/L). Note that this TTHM value is close to the MCL of TTHM by Stage 2 D/DBPR.

At sampling site #23, it was observed that a slight red color was noticeable in the sample collected immediately after the fire hydrant was opened. The iron concentration in the water collected after 10 min of flushing was 4.9 mg/L, which was more than an order of magnitude higher than the average iron concentration (0.45 mg/L) throughout the distribution system. Therefore, a severe corrosion and resulting reductive loss of chlorine by ferrous iron might be responsible for low residual in this location.

At sampling location #32, the residual chlorine and HAA5 concentrations were almost zero. Interestingly, some air bubbles were observed to evolve in the water as samples were collected. The HPC of the sample analyzed was 175 cfu/mL, which was much higher than the HPC values normally observed in the drinking water distribution system. It is possible that microbial activity is relatively high at this location, which accelerated chlorine decays and HAA5 biodegradation. In addition, this sampling site was located near a Bogan Road water storage tank and the pipeline was dead-end. Therefore water age was relatively longer compared with ones at the other areas, which also affected the TTHM concentration (55.2 µg/L).

As residual chlorine was closely associated with DBP formation, additional analyses to evaluate these relationships were performed. In particular, the change in TTHM concentration (= \*TTHM Concentration) was compared with the change in residual chlorine (= \*Residual

Chlorine) in Figure 11. These changes were defined as the difference between the concentration at the sampling point and the concentration at the finished water on the same day. It is apparent that the greater the decay of chlorine, the greater the increase in TTHM.

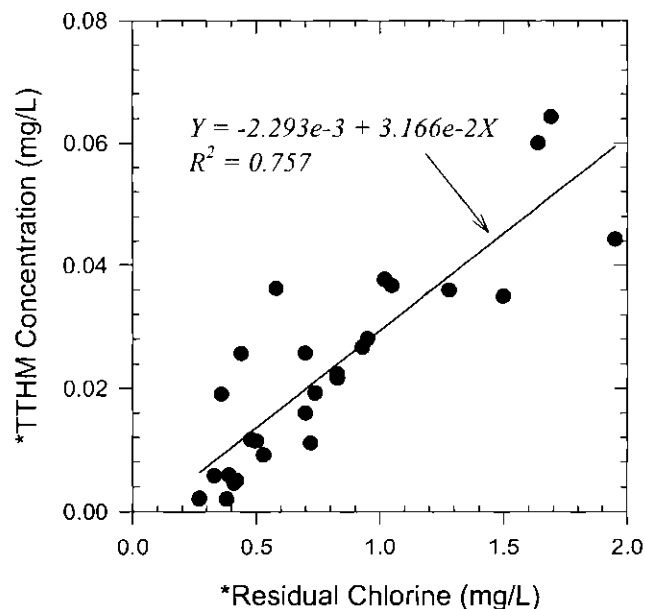


Figure 11. Comparing differential TTHM concentration and differential residual chlorine

A relationship between differential HAA5 concentration and different residual concentrations were also examined in Figure 12. And it was found that overall the HAA formation increased as residual chlorine concentration decreased, while scattering of the data was significant and it might not be appropriate to claim a linear relationship. Some decrease in HAA concentrations at higher differential residual chlorine (*i.e.* longer retention time and lower chlorine residual) was also apparent. Greater deviations from the linearity might have been caused by the effect of microbial activity in the distribution system on HAA degradation, which is enhanced at low chlorine concentration.

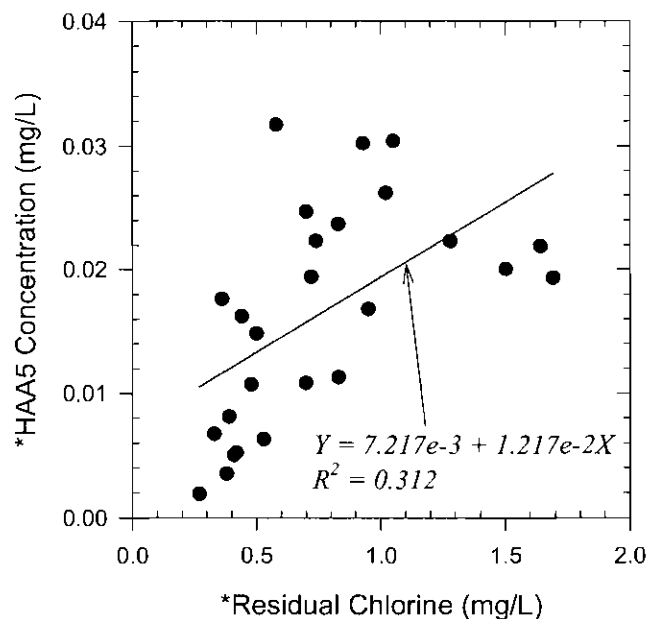


Figure 12. Comparing differential HAA5 concentration and differential residual chlorine

Some regulatory standards including D/DBPR are based on the sum of the concentrations of a few representative species. However, as widely varying levels of adverse health effects are identified for different individual DBP species, a regulatory approach based on each individual compound rather than the sum of the classes has been under discussion. For example, the World Health Organization suggests different MCLs for each of the four THM species (World Health Organization, 2005). The MCLs of chloroform, bromodichloromethane, dibromochloromethane, and bromoform are 300 µg/L, 60 µg/L, 200 µg/L, and 100 µg/L, respectively. In Figures 13 and 14, differential concentrations of individual THM and HAA species were compared to the differential residual chlorine. It was observed that chloroform represented the largest portion of the TTHM among the four THMs. In addition, bromoform concentration was below detection limit in all the samples, which is likely due to the historically low concentrations of bromide present in Lake Lanier source water and is consistent with the lack of a bromate formation problem with the use of pre-ozonation processes at LFP and SCFP. Similar to TTHM, there was also a linear increase in the concentrations of chloroform, bromodichloromethane, and dibromochloromethane as the concentration of residual chlorine decreased. As for the HAA5,

monohaloacetic acid, dichloroacetic acid, and trichloroacetic acid were major species while the other two species, bromoacetic acid and dibromoacetic acid, were not detected.

The relationship between the concentration of these species and residual chlorine concentration was less apparent, as data largely scattered.

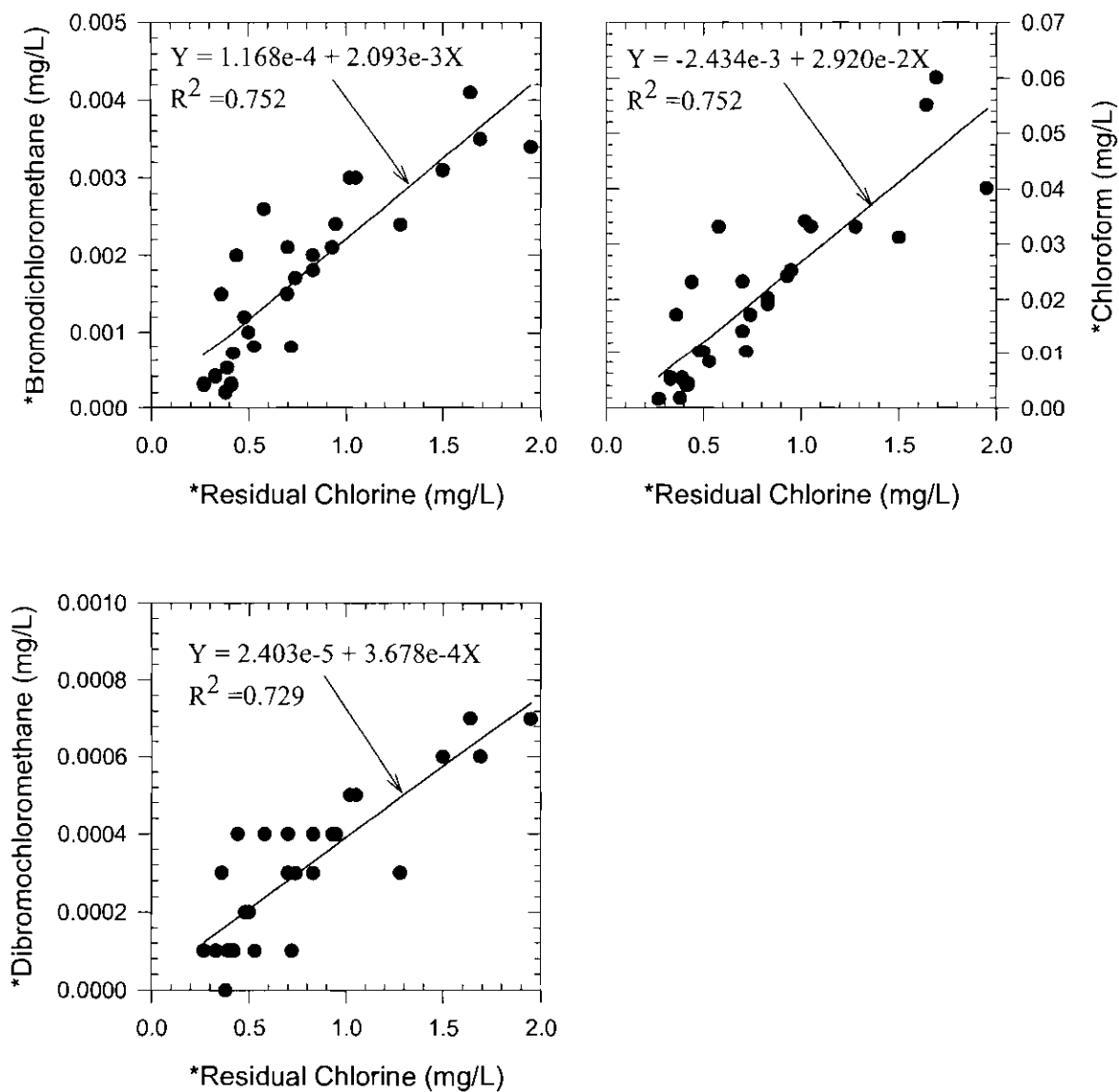


Figure 13. Comparing differential THM concentration and differential residual chlorine



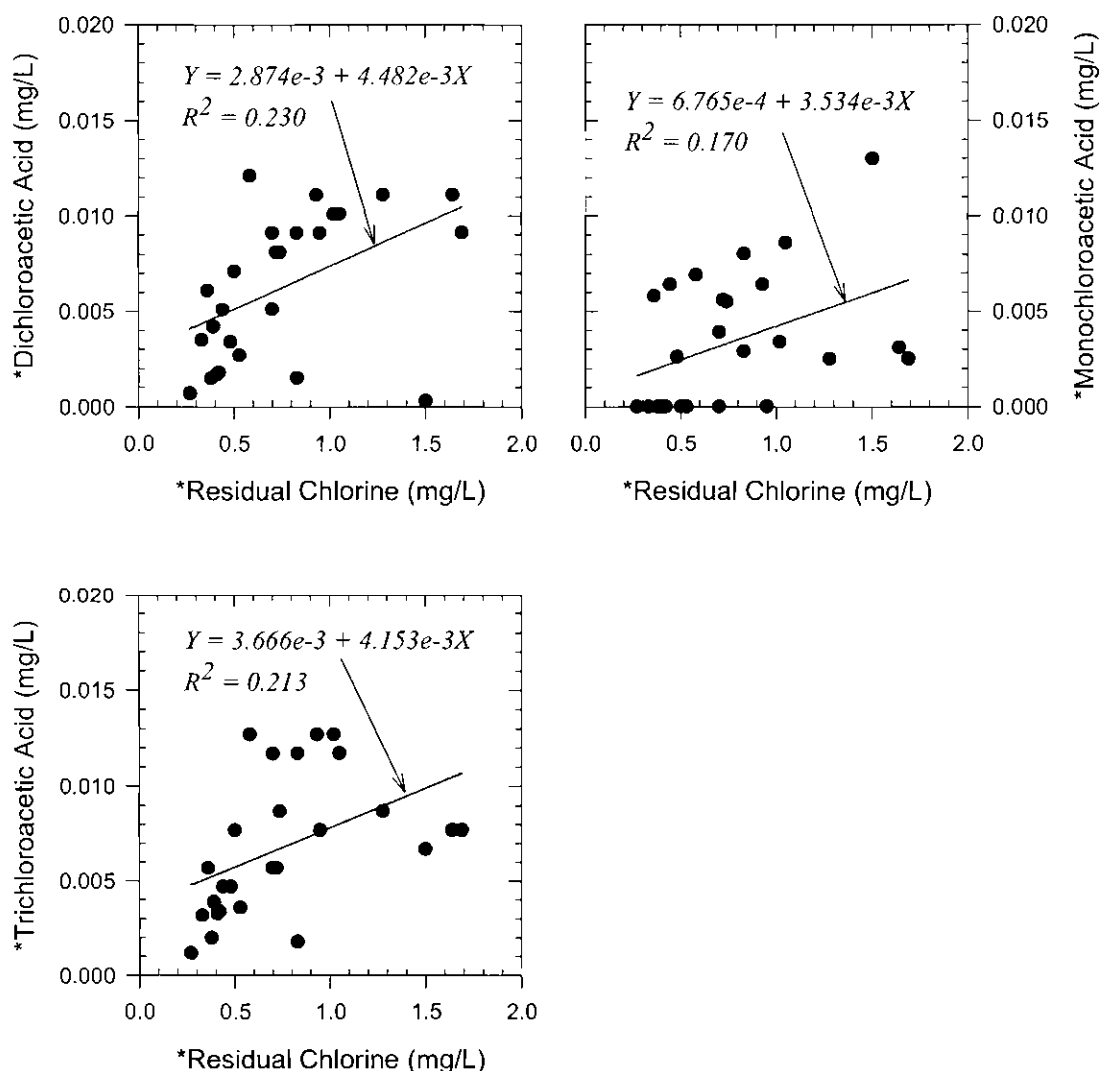


Figure 14. HAA species concentration vs. residual chlorine concentration

Natural organic matter (NOM) is the precursor for the formation of both THMs and HAAs. Figures 15 to 18 show the relationships between water quality parameters such as TOC, DOC,  $UV_{254}$  and SUVA and THM and HAA formation. It appeared that these parameters did not change much throughout the distribution system and therefore no meaningful relationships were derived. How NOM changes affect the DBP formation in the distribution system was not

discernable based on this analysis. Nonetheless, the real utility of SUVA, TOC, and DOC data is in modeling DBP formation kinetics and being able to compare the results obtained in Gwinnett County with results obtained elsewhere. The nature and concentration of NOM would not be expected to change significantly in the distribution system, but these parameters do tend to vary significantly between locations across the country and significantly impact the formation of DBPs in all cases.

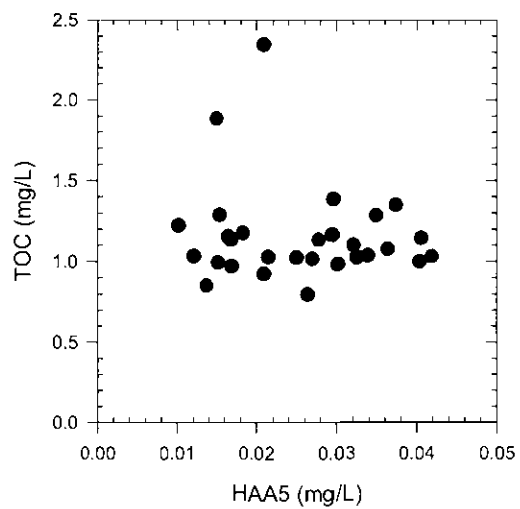
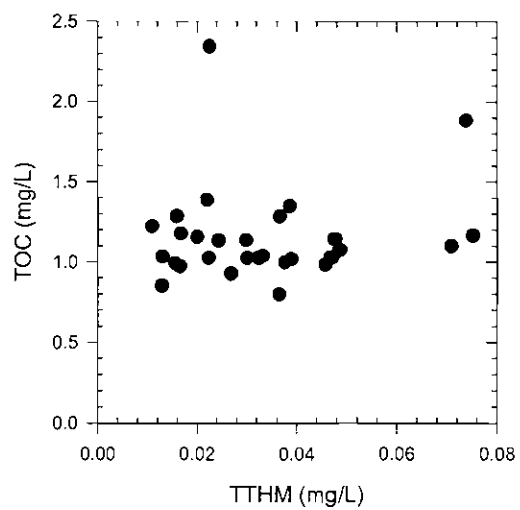


Figure 15. TOC vs. TTHM or HAA5 concentration

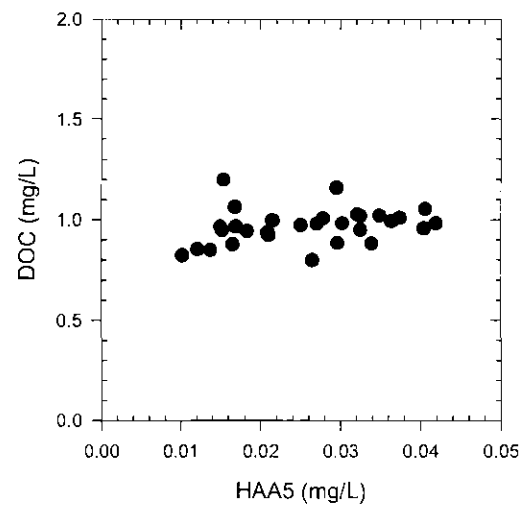
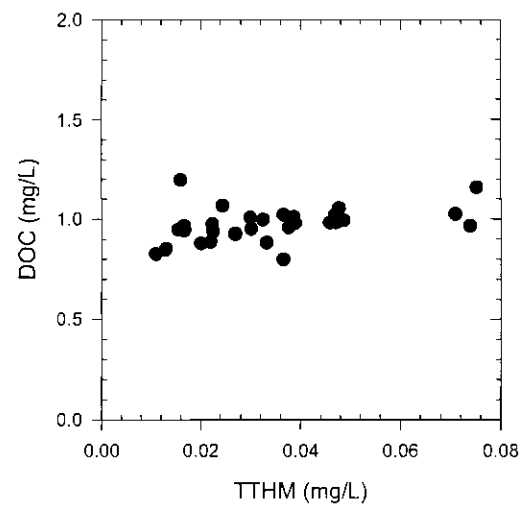


Figure 16. DOC vs. TTHM or HAA5 concentration

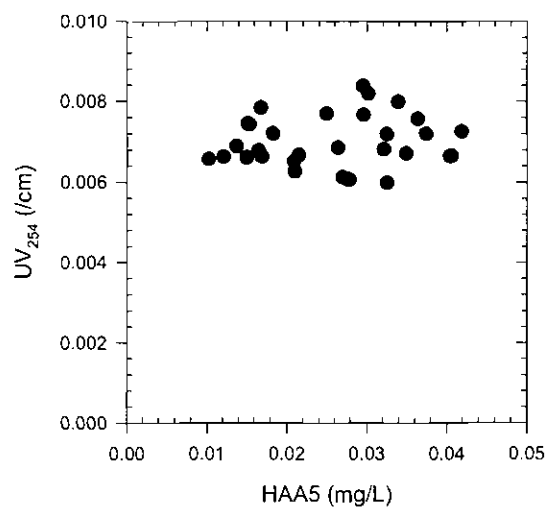
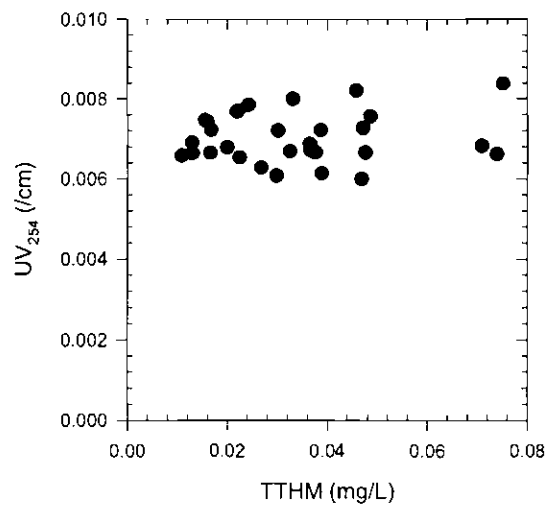


Figure 17. UV<sub>254</sub> vs. TTHM or HAA5 concentration

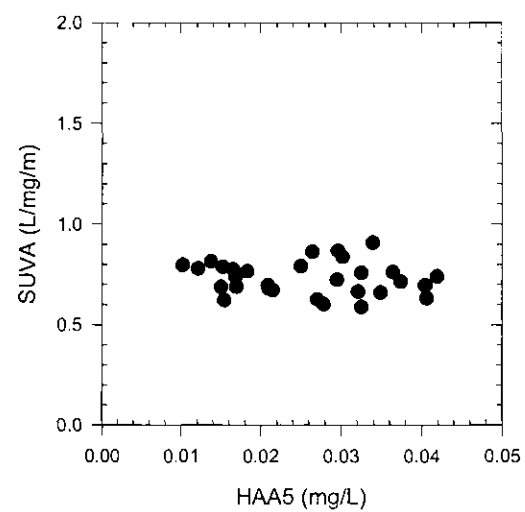
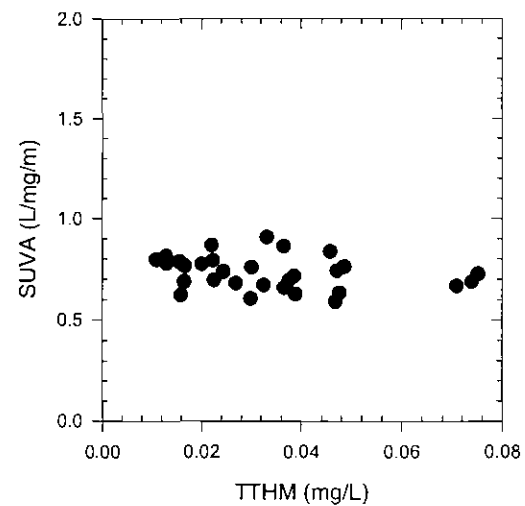


Figure 18. SUVA vs. TTHM or HAA5 concentration

### 3.3. Batch Kinetic Study

Figure 19 shows the decay kinetics of free chlorine at 25°C determined from the laboratory batch experiments. The data was fitted using a first-order decay model ( $dC/dt = -kt$ ). When integrated,  $C_t = C_0 \cdot \exp(-kt)$ , where  $C_t$  = chlorine concentration (mg/L) at time  $t$ ;  $C_0$  = initial chlorine concentration (mg/L) ( $t=0$ );  $k$  = the first-order rate constant ( $1/d$ ). From the curve fitting, the rate constant was determined at  $0.1039 \text{ d}^{-1}$ . This first-order decay rate was used for the simulation of the residual chlorine concentration by WaterGEMS. Note that the rate of chlorine decay determined from the laboratory batch experiments would be less than actual decay in the distribution system, since additional chlorine decay results from reaction with the pipe wall (surface or corrosion products) and biofilm.

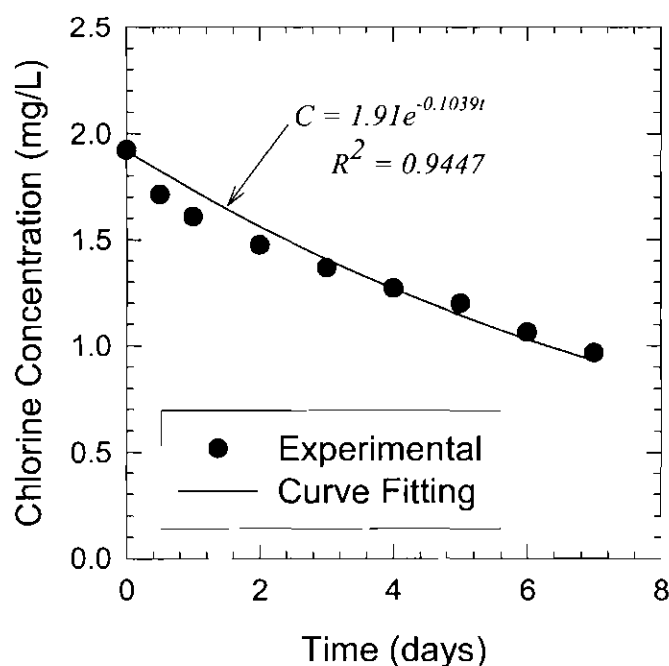


Figure 19. Kinetics of residual chlorine decay at 25°C in a laboratory batch experiment

Figures 20 and 21 show the kinetics of TTHM and HAA5 formation at 25°C also determined from the laboratory batch experiments. The solid lines represent the fitting of the

experimental data with the equation,  $C_t = C_L - (C_L - C_0) \cdot \exp(-kt)$ , where  $C_t$  = DBP concentration at time  $t$  ( $\mu\text{g/L}$ );  $C_L$  = limiting concentration ( $\mu\text{g/L}$ ), which is the maximum concentration found during 7-day test;  $C_0$  = the initial DBP concentration ( $\mu\text{g/L}$ ) (*i.e.*  $t = 0$  or finished water); and  $k$  = first-order rate constant. The initial concentrations of TTHM and HAA5 were  $10.9 \mu\text{g/L}$  and  $10.2 \mu\text{g/L}$  and the rate constants ( $k$ ) were determined from the curve fitting at  $0.325 \text{ d}^{-1}$  and  $0.143 \text{ d}^{-1}$ , respectively for THM and HAA.

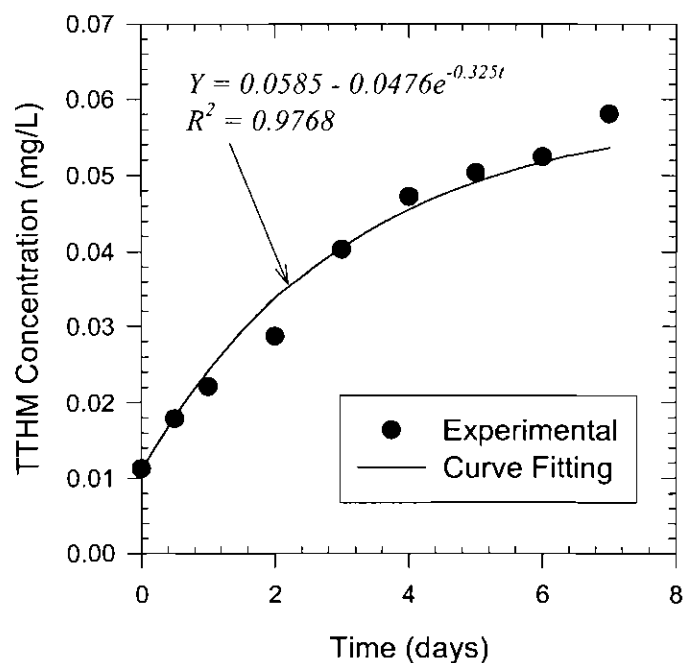


Figure 20. Kinetics of TTHM formation at 25°C in a laboratory batch experiment

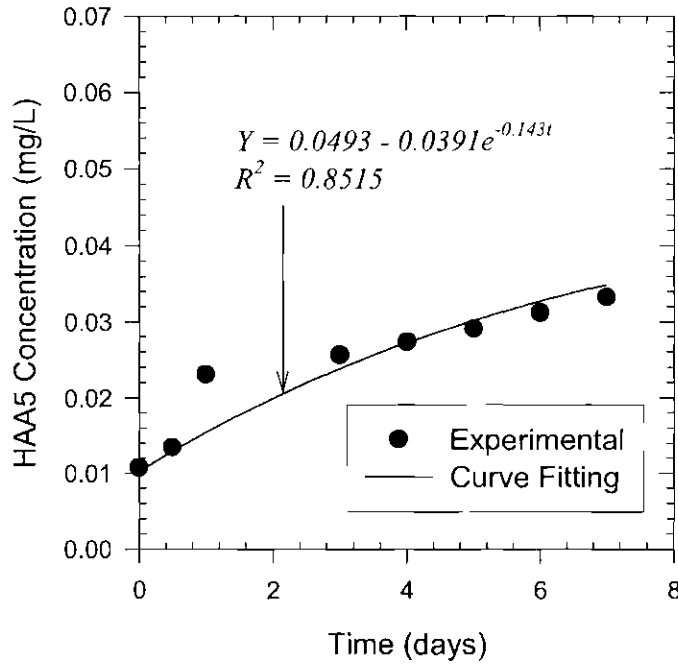


Figure 21. Kinetics of HAA5 formation at 25°C in a laboratory batch experiment

### 3.4. Water Quality Simulation

The water distribution system model that was validated with tracer tests in this study was used to simulate water quality in the distribution system. The modeling was performed to simulate the water age with the average daily demand of 79.1 MGD (*i.e.* water demand on the date of field study). The simulation was run for an elapsed time of 312 hours at 1-hour increments to achieve an extended period simulation (EPS). The initial values for the residual chlorine, TTHM and HAA5 were determined from the field measurement. The DBP formation potential (DBPFP) determined from separate bench-scale experiments were taken as the limiting concentrations for TTHM and HAA5 formation. In addition, the rate constants for chlorine decay and DBP formation determined from the batch kinetic tests were also used. It was assumed that the chlorine-wall reaction rate constant would be inversely proportional to the *Hazen-Williams C-factor* for each pipe segment, *i.e.* a wall reaction coefficient,  $k_w = F/C$ , where

$F$  = wall reaction-pipe roughness coefficient. The  $C$  factor of each pipe in the model had previously been assigned based on the pipe ages, materials, and field data obtained for the model calibration. The actual boundary conditions of the distribution system were assigned to the model as appropriate.

Figure 22 shows the simulation result on the spatial distribution of residual chlorine in color-coded time increment. The residual concentrations in most locations in the distribution system were higher 1.0 mg/L. Consistent with the previous discussions based on tracer tests and corresponding model simulations, the south and east extremities exhibited the lowest residual chlorine concentrations as water travels for longest period to reach those areas. The calculated residual chlorine levels under the optimum modeling conditions (*i.e.*  $F = 1.0$ , best fit with the field data) were compared with ones obtained from the field measurement (Figure 23). It was found once again that the calculated residual chlorine concentration obtained from the computational modeling agree well with the measured data especially at higher concentrations. However, the model accuracy gradually decreased as the chlorine concentration decreased and water age increased.



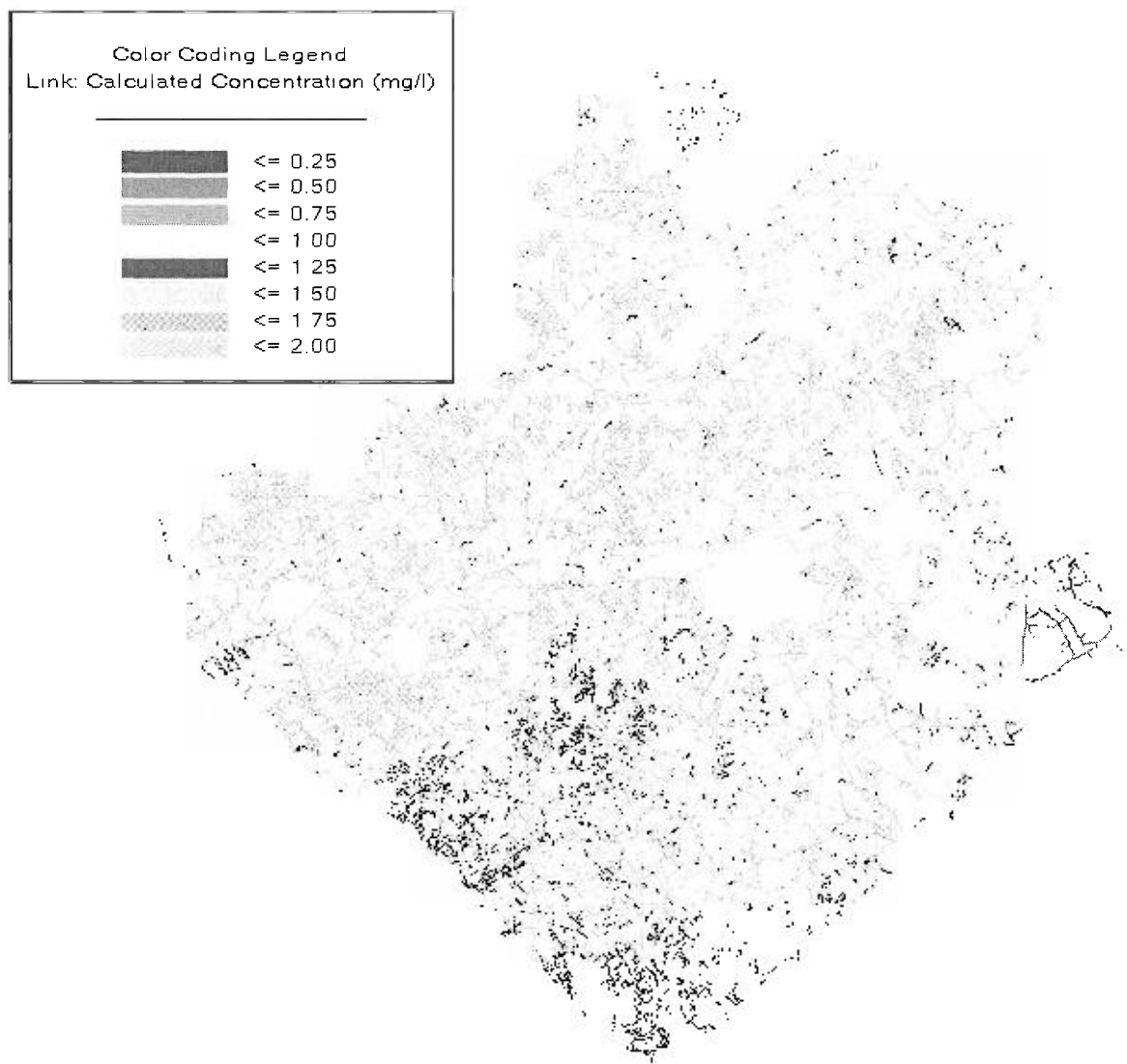


Figure 22. Model simulation of residual chlorine concentration in the Gwinnett County water distribution system (under the condition for the date of field experiment)

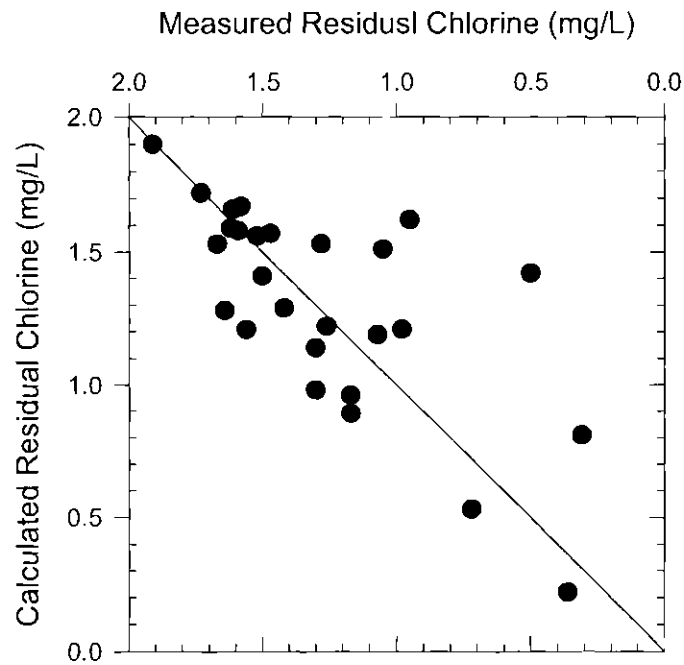


Figure 23. Comparing residual chlorine measured in the field and predicted with the model.

TTHM and HAA5 concentration were also predicted from the same simulation and the results were compared with the experimental data in Figures 24 and 25. While accuracy of the prediction varied somewhat with the input parameters, it was found that the best fits for TTHM and HAA5 were obtained when wall effects were assumed negligible (*i.e.*  $K = 0$ ). This suggests that the model might have over-predicted the DBP concentrations, probably due to (1) inappropriate C factor values assigned to each pipe, (2) the overestimated DBP kinetic rates in bulk water, and (3) negligible wall effect in reality. Currently, it is impossible to accurately assign all the wall effect in such a large network system.

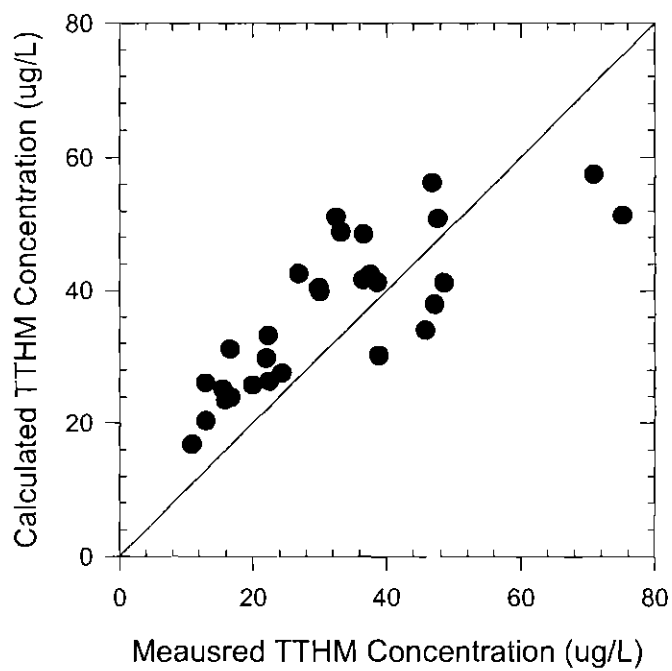


Figure 24. Comparing TTHM measured in the field and predicted with the model

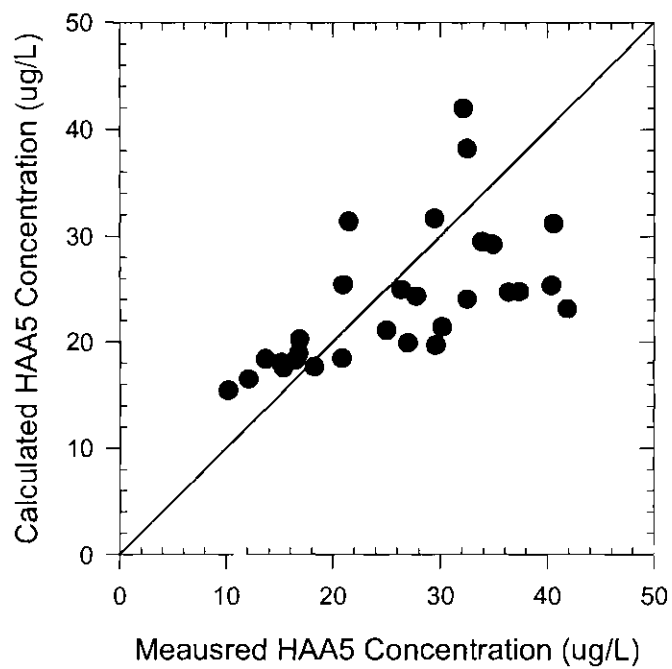


Figure 25. Comparing HAA5 measured in the field and predicted with the model

#### 4. CONCLUSIONS

The following summarizes the major conclusions from this part of study:

1. The distribution system model fairly accurately simulated the water ages determined by the conservative tracer test results.
2. Water age was an important indicator used to determine water quality in terms of both chlorine residual and TTHM levels in this distribution system. A less reliable linear relationship with HAA5 might have resulted from contribution of microbial degradation in the distribution system.
3. TTHM formation showed a relatively linear relationship with the amount of free chlorine residual decayed. A less reliable linear relationship with HAA5 might have resulted from contribution of microbial degradation.
4. The regions within the distribution system with the longest retention time and lowest free chlorine residuals were identified from both modeling and field study. In Gwinnett County, the east-most and south-most boundary areas were identified as problematic regions.
5. Several water quality parameters including TOC, DOC,  $UV_{254}$ , and SUVA were examined but no apparent relationship with residual chlorine decay and DBP formation was observed. However, these parameters are important when attempting to interpret Gwinnett County's results with those of other water systems.
6. DBP concentrations of all the samples measured from the field measurement were below than MCLs imposed by the Stage 2 D/DBPR.
7. Chloroform represented the largest portion of the TTHM among the four THMs, while bromoform concentration was below detection limit in all the samples. As for

the HAA5, monohaloacetic acid, dichloroacetic acid, and trichloroacetic acid were major species while the other two species, bromoacetic acid and dibromoacetic acid, were not detected.

8. A few sampling locations showed abnormality in free chlorine residual, DBP concentrations, and other water quality parameters (pH and iron concentration). Extended retention in water storage tank, presence of dead-end pipes, excessive microbial activity, and pipe-wall corrosion might be related, while further studies would be necessary to determine exact causes.

Based on knowledge obtained in this project, the following might need to be considered for future research efforts.

1. As operating conditions of storage tanks might significantly affect water quality parameters, they need to be carefully evaluated to avoid the problems observed in this study, for example, water retention for an extended period and excessive loss of chlorine residual.
2. It is nearly impossible to accurately estimate wall coefficients for all the pipes in a very large distribution system such as Gwinnett County because complex and heterogeneous conditions exist inside each pipeline. However, it may be still worth performing some field tests to evaluate the C factors, especially in the regions with problematic water quality. An extensive sensitive analysis of the distribution system might need to be performed to minimize the discrepancy between the calculated and the measured water quality.
3. Pipe corrosion and excessive microbial activity in some parts of the distribution systems were identified and further study might be necessary to identify the reasons and propose appropriate solutions.

**PART II.**  
**DEVELOPING A NOVEL OZONE- MEMBRANE HYBRID PROCESS**  
**FOR LANIER FILTER PLANT**

## 1. INTRODUCTION

Low-pressure membrane processes such as microfiltration (MF) and ultrafiltration (UF) are widely used in drinking water treatment for removal of pathogenic microorganisms such as bacteria and protozoa (e.g., *Cryptosporidium parvum*) as well as particulate and colloidal contaminants. The removal of natural organic matter (NOM) has been another treatment goal, because NOM contributes to color, taste, and odor in the product water, provides a nutrient for bacterial regrowth in a distribution system, and associates with pesticides and heavy metals, thus facilitating their transport through a distribution system. Even more importantly, NOM serves as a precursor during chlorination for disinfection by-products such as trihalomethanes, haloacetic acids, etc.

A major obstacle for the MF and UF process has been membrane fouling, which is responsible for decreases in permeate production rate and increases in operational costs. In many applications, accumulation of NOM on the membrane surface as a form of gel layer and adsorption of NOM on the membrane surface and inside the membrane pores have been identified as primary causes for membrane fouling. Gel layers and loosely-bound NOM are relatively easily removed by physical cleaning methods such as periodic back-flushing. However, organic matter that are strongly adsorbed on the membrane surfaces are not readily removed by physical methods, and only up to a certain degree by chemical cleaning. A portion of membrane fouling is, therefore, irreversible and cause a long-term irrecoverable performance deterioration and eventually a need for replacing membrane units.

Chemicals such as free chlorine and caustics have been used to remove organic matter that is strongly bound to membrane and recover the permeate production rate. The chemical cleaning agents act by breaking the physical and chemical bonds, through oxidation and hydrolysis, between the organic matter and the membrane surface. Therefore, it is possible that stronger oxidant such as ozone would be more effective. Ozone is a very strong oxidant used in disinfection and advanced oxidation processes. A secondary oxidant such as hydroxyl radical, which is even stronger oxidant than ozone, is produced as a result of ozone self-decomposition and reaction with chemicals such as hydrogen peroxide that is added in advanced oxidation

processes. It is recognized that ozone makes NOM more hydrophilic by oxidizing saturated carbon to produce functional groups such as aldehydes and carboxylic acids (Westerhoff *et al.*, 1999), while hydrophobic interactions are likely to be responsible for irreversible fouling. Therefore, it is presumed that ozone may be effective in preventing the formation of membrane fouling, when it is introduced in the feed, as well as cleaning a membrane fouled with NOM.

Use of even much weaker oxidant such as chlorine to clean the fouled membrane has been limited due to possible damage to the polymeric structure of the membranes. An alternative approach of making use of a strong oxidizing power of ozone in a membrane process is to use chemically-inert ceramic membranes instead of polymeric membranes. Ceramic membranes are recently considered as a promising alternative in drinking water production (Bottino *et al.*, 2001), since they exhibit not only superior chemical and physical strength but better structural integrity and much longer lifetime compared to polymeric membranes. A major limitation of the ceramic membranes has been high costs during initial installation, even though replacement costs are much lower than polymeric membranes. With decrease in membrane material costs, overall cost of ceramic UF processes have significantly decreased in recent years, while they might not yet be competitive to polymeric membranes at this moment.

The objective of this project was to investigate an alternative treatment option of employing a ultrafiltration (UF) membrane process in place of conventional media filtration currently in use in the Lanier Filter Plant (LFP) in Gwinnett County, GA. As the LFP is currently practicing the pre-ozonation, the study focused on identifying benefits of installing a ceramic UF membrane process coupled with existing ozonation process, with the ultimate goal of obtaining a synergism in pathogen removal and membrane fouling mitigation. Fouling characteristics of a commercial ceramic UF membrane treating LFP source water and water after ozonation were investigated using a laboratory-scale cross-filtration setup. A resistance-in-series model was applied to understand the mechanism of fouling. Finally, the feasibility of ceramic UF membrane process for the LFP is discussed.



## 2. MATERIAL AND METHODS

### 2.1. Feed Water

The Lake Sidney Lanier, formed by holding the Chattahoochee and Chestatee Rivers, encompasses *ca.* 38,000 acres and provides the source water for the LFP. The water quality is known to be relatively stable and characterized by low suspended solids, dissolved organics and metal contents. Water samples for the experiments was taken before (pre-ozonation) and after (post-ozonation) ozone contactor #2. Table 8 below shows the typical water quality parameters for the raw water.

Table 9. Characteristics of LFP source water used in this study

<i>Parameters</i>	<i>Values</i>
TOC (mg/L)	1.3 - 2.5
pH	6.5 - 7.5
Nitrates (mg/L)	0.2 - 0.23

### 2.2. Membranes

A tubular silica ceramic membrane with nominal molecular weight cut-off (MWCO) of 50K along with a custom-fit module were obtained from Ceramem Corp. Physical specifications of this membrane include: diameter = 27 mm; length = 305 mm; channel diameter = 2 mm, the number of flow channels = 60; active membrane surface area = 0.13 m<sup>2</sup>; and cross flow area = 2.17 cm<sup>2</sup>. The manufacturer's specifications for the operating conditions of the membrane and the module are: maximum temperature = 130°C; maximum transmembrane pressure = 150 psi; recommended cross-flow velocity = 3 to 4 m/s; membrane area = 0.13 m<sup>2</sup>; pressure drop of water at maximum velocity = 6.5 psi (0.45 bar ) at 25°C.

### 2.3. Cross-Flow Filtration Experiments

Flow-through experiments were performed for tubular ceramic membranes. Photographs and a schematic of the experimental setup is shown in Figures 26 and 27. The membrane was housed in a stainless steel cylindrical sanitary module with tri-clamp sealed inlet/outlet. This unit was located in the basement of ozonation facility in the LFP such that a large volume of real water was used for the filtration experiments.

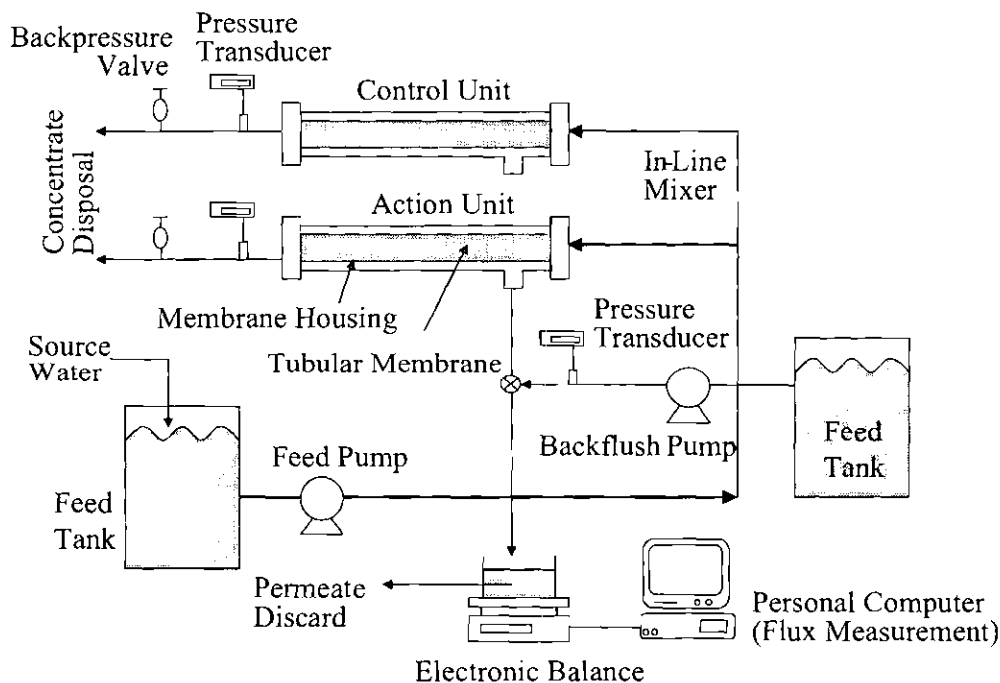
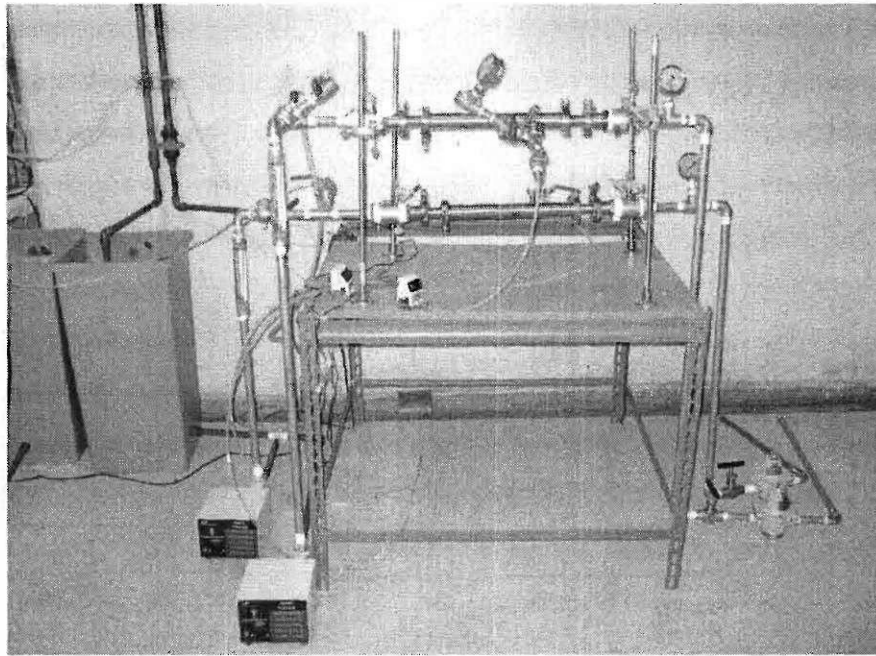
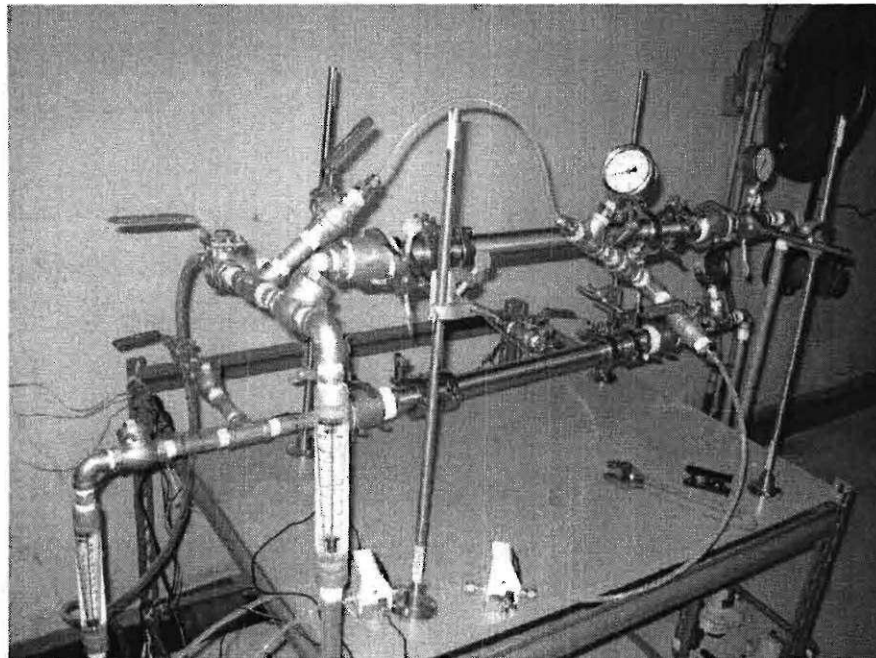


Figure 26. Schematic of Crossflow Filtration Experimental Setup

In order to examine the effect of ozonation on filtration performance, two modules were operated in parallel - one module (the control unit) treating ozone contactor influent (*i.e.* reservoir water before ozonation) and the other module (action unit) treating the effluent from the ozone contactor. Each water sample was collected from a pipe connected to the contactor influent and effluent line in the contactor room into each of two 13-gallon drums. Each water sample was pumped by a variable speed centrifugal pump (Model 75211-62, Cole-Parmer Co. Chicago, Illinois, 0.13 HP, 90 ~ 9000 rpm) into each membrane module. Feed flow rate was controlled by adjusting the pump rotation speed and a flow control valve and determined by a flow meter (F-400, Blue White Industries, Ltd.) located downstream of the module. Influent



(a) Front view of experimental setup



(b) Experimental setup during membrane backwashing

Figure 27. Photographs of Experimental Setup

flow rate and cross-flow velocity were 9.0 LPM and 0.69 m/s, respectively. Feed pressure was controlled at 15.0 psi by adjusting a back pressure valve located downstream of concentrate line. Temperature of the feed waters was not controlled but was relatively constant at 19.0 to 19.5°C. The permeate flux was monitored by measuring the volume of permeate in a graduated cylinder over a specified time interval.

#### **2.4. Membrane Cleaning.**

Four different methods were used to clean the fouled ceramic membranes after the completion of filtration experiment; chemical cleaning, mechanical cleaning, backwashing and ozone treatment. A chemical cleaning of the fouled membranes (after completion of filtration experiments) were performed by soaking them in a 2 % citric acid solution (pH = ~2.0) and 500 mg/L NaOCl (pH = ~9.0) solution in series. Both cleanings were conducted at 55°C for 2 hrs. After each cleaning, the membrane was rinsed with distilled water. A mechanical cleaning was performed by increasing the influent flow rate by two times with blocking the permeate flow line and completely opening the back-pressure valve for 2 hours. Backwashing was performed by injecting distilled water through a permeate line at 15.0 psi for 10 min. A flow line from a water storage tank to the permeate line was added and the same pump used for feed flow was used for backwashing. A pressure gauge was installed before the module. Ozone treatment was performed by soaking the membrane in a solution of 5.0 mg/L of ozone for 20 min. The concentration of ozone was maintained at constant by continuously bubbling ozone gas produced from pure oxygen through a gas diffuser.

The effectiveness of each cleaning procedure was verified by measuring the permeate flux using distilled water. The operating conditions were the same as those of cross-flow filtration experiments. (influent flow rate = 9.0 LPM, cross flow velocity = 0.69 m/sec, pressure = 15.0 psi, temperature = 19.0 ~ 19.5°C)

#### **2.5. Analytical Methods.**

Total organic carbon (TOC) was analyzed by a Shimazu TOC-V analyzer. SUVA was determined by dividing the UV absorbance of the sample (in  $\text{cm}^{-1}$ ) by the TOC of the sample (in  $\text{mg/L}$ ) and then multiplying by 100  $\text{cm/M}$ . UV absorbance at 254 nm was measured using a Agilent 8453 UV-Vis spectrophotometer.

### 3. RESULTS AND DISCUSSION

Permeate flux changes over filtration time of 96 hours (4 days) are shown in Figure 28. It is apparent that there is little difference between the membrane feed water before and after ozonation. In both cases, the permeate flux rapidly decreased from the initial value of *ca.* 120 LMH ( $\text{L/m}^2\text{-hr}$ ) at the initial stage of filtration and reached the steady-state flux of *ca.* 20 LMH after 3 days. Overall permeate flux decrease was *ca.* 83%.

Figures 29 and 30 show the representative water quality parameter change during filtration (TOC in Figure 29 and Specific UV absorbance in Figure 30). It is noteworthy that there was again little difference between the ceramic membrane treating ozone contactor influent and effluent. Also note that permeate water quality reached its steady-state value much faster

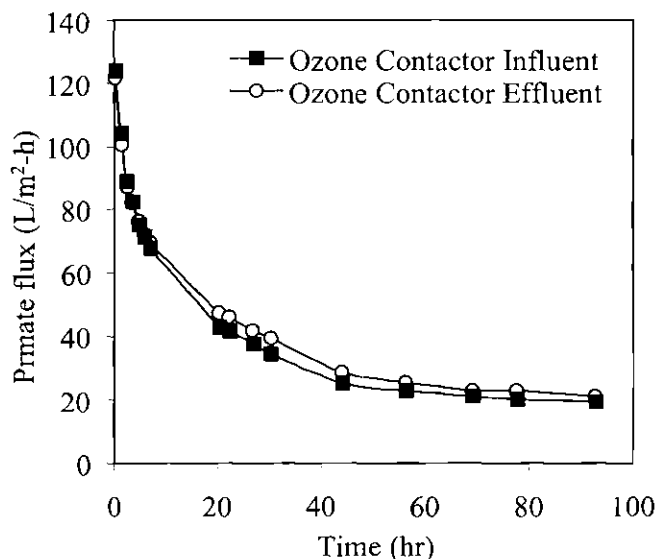


Figure 28. Permeate fluxes of ceramic membranes treating ozone contactor influent and effluent.

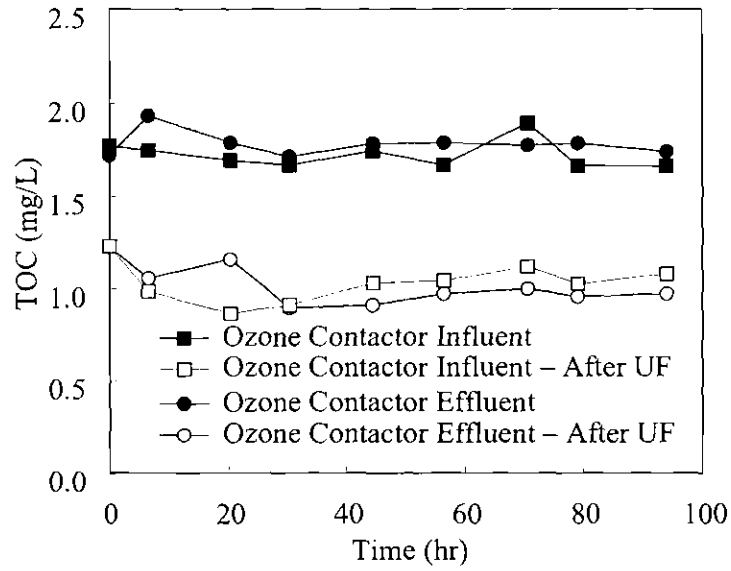


Figure 29. Total organic carbon in membrane feed and permeate.

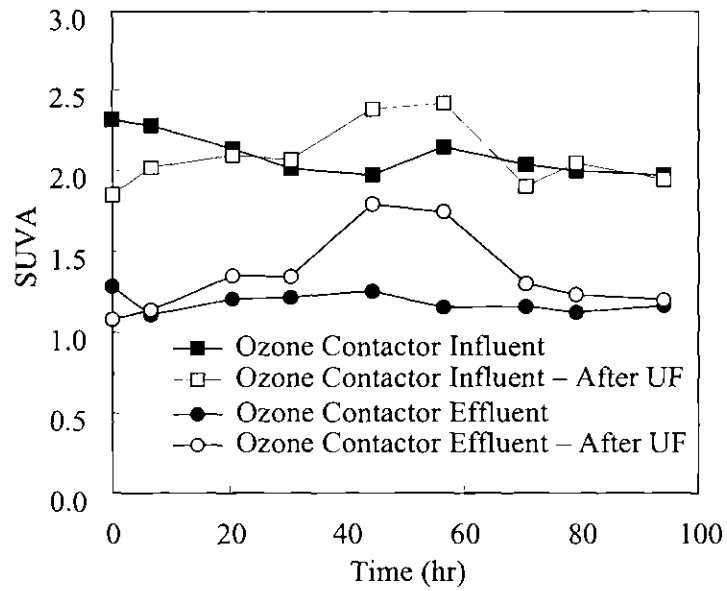


Figure 30. Specific UV absorbance of membrane feed and permeate.

than permeate flux. The rejection is defined as follows:

$$R = 1 - \frac{C_P}{C_F} \quad (1)$$

where  $C_p$  and  $C_f$  = Permeate and feed concentrations, respectively. The steady-state rejection was approximately at 35-45 % in terms of TOC. SUVA values showed some scattering and no meaningful conclusions could be drawn.

At the end of the filtration, membranes were cleaned following four different methods described above and permeate fluxes using distilled water were measured at the same operating conditions. Table 10 summarizes the experimental results.

Table 10. Permeate flux at each stage.

Membrane	Flow rate	Initial	After Fouling	After Mechanical	After Chemical	After Backwash	After Ozone
Ozone Contactor	Flow rate (ml/min)	360.0	41.8	61.8	106.1	105.5	113.0
Influent	Specific Flux (LMH/bar)	160.7	18.7	27.6	47.4	47.1	50.5
Ozone Contactor	Flow rate (ml/min)	377.3	47.2	89.8	133.5	148.1	165.2
Effluent	Specific Flux (LMH/bar)	168.4	21.1	40.1	59.6	66.1	73.8

These data were analyzed using a resistance-in-series model. According to resistance-in-series model, the volumetric flux  $J_v$  during membrane filtration can be expressed as follows:

$$J_v = \frac{\Delta P}{\mu R_T} \equiv \frac{\Delta P}{\mu(R_M + R_C + R_F)} \quad (2)$$

Where  $J_v$  = Permeate Flux ( $\text{LT}^{-1}$ );  $\Delta P$  = Trans-membrane pressure;  $\mu$  = Viscosity of the liquid;  $R_T$  = Total resistance;  $R_M$  = Resistance of the membrane;  $R_C$  = Resistance from cake (gel layer) formation; and  $R_f$  = Resistance from adsorbed irreversible fouling.

Note that cake resistance consists of *ca.* 32% and 48% of total resistance of the membrane after treating ozone contactor influent and effluent, respectively (Figure 31). Accordingly, irreversible fouling consisted of 56% and 40% of total resistance for the membrane treating ozone contactor influent and effluent. It is interesting that relative contribution of irreversible fouling decreased as the source water was treated with ozone. Consistently, the membrane which treated ozone contactor effluent was cleaned more efficiently than the membrane that treated ozone contactor effluent, especially through the mechanical cleaning (Table 10).

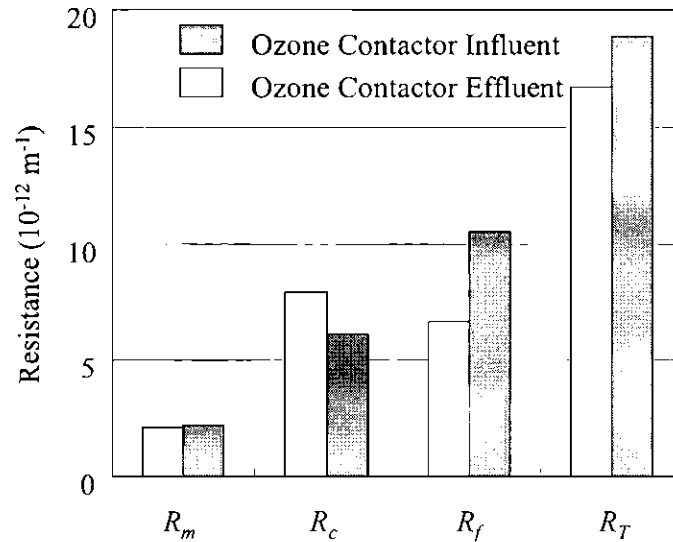


Figure 31. The calculated resistances of two membranes from resistance in series model

Additional ozone treatment, unfortunately, did not result in an appreciable level of permeate flux increase, in contrast to hypothesis of the project. Instead, ozone treatment showed



a marginal performance increase compared to chemical treatment using acid and base. If the permeate flux were to be significantly improved by ozone treatment, we could have performed a few additional experiments including 1) in-line ozone gas injection into the feed line and 2) backwashing with ozone solution. Based on the fact that an extensive ozone treatment (in a semi-batch mode with  $CT = 100 \text{ mg-min/L}$ , which is unrealistically high for any full-scale operation) did not result in any substantial increase in permeate flux, these additional tests were considered meaningless.

#### 4. CONCLUSIONS

Results obtained from this study suggested the following:

1. Ozone treatment of raw water did affect the fouling characteristics of UF membrane. After ozone treatment, the overall contribution of cake resistance to the total resistance increased. However, little difference was observed with the total resistance. We suspect that ozonation induced oxidation of some of NOM such that a fraction of NOM became hydrophilic and bound to the membrane surface in a more reversible way, while the total NOM amount that participated in membrane fouling through either cake formation or irreversible fouling did not change. This finding might be valuable when the LFP considers membrane process for future plant upgrade, as it will affect membrane operation options such as mechanical and chemical cleaning methods and frequency.
2. Unfortunately, a direct application of ozone to the fouled membrane was found not very effective, when compared with commonly used chemical treatment methods. This suggested that irreversible fouling observed with the ceramic membrane might have resulted from pore clogging, which is not easily removed by either mechanical or chemical methods.
3. As the major advantage of using the ceramic membrane is its extremely strong chemical resistance and potential for cleaning by the existing ozonation facility, this suggests that the use of high-cost ceramic membrane might not be justifiable at the LFP.

## 5. REFERENCES

- Bottino, A.; Capannelli, C.; Del Borghi, A.; Colombino, M.; and Conio, O. (2001). "Water treatment for drinking purpose: ceramic microfiltration application." *Desalination*, 141, 75-79.
- Westerhoff, P.; Debroux, J.; Aiken, G.; Amy, G. L. (1999). "Ozone-Induced Changes in Natural Organic Matter (NOM) Structures." *Ozone Science and Engineering*, 21, 551-570.
- Archer, A. D., and Singer, P. C. (2006). "An evaluation of the relationship between SUVA and NOM coagulation using the ICR database." *Journal / American Water Works Association*, 98(7), 110-123.
- Chen, W. J., and Weisel, C. P. (1998). "Halogenated DBP concentrations in a distribution system. With increasing residence time, concentrations of THMs increased, but concentrations of HANs, HKs, CP, and HAAs decreased." *Journal / American Water Works Association*, 90(4), 151-163.
- Digiano, F. A., and Zhang, W. (2005). "Pipe section reactor to evaluate chlorine-wall reaction." *Journal / American Water Works Association*, 97(1), 74-85.
- Harding, B. L., and Walski, T. M. (2000). "Long time-series simulation of water quality in distribution systems." *Journal of Water Resources Planning and Management*, 126(4), 199-209.
- Pereira, V. J., Weinberg, H. S., and Singer, P. C. (2004). "Temporal and spatial variability of DBPs in a chloraminated distribution system." *Journal / American Water Works Association*, 96(11), 91-102.
- Rossman, L. A., Brown, R. A., Singer, P. C., and Nuckols, J. R. (2001). "DBP formation kinetics in a simulated distribution system." *Water Research*, 35(14), 3483-3489.